AD 453901

NWL Report No. 1950

EXPLOSIVE HARDENING OF IRON AND LOW-CARBON STEEL

by

L. A. Potteiger
Warhead and Terminal Ballistics Laboratory

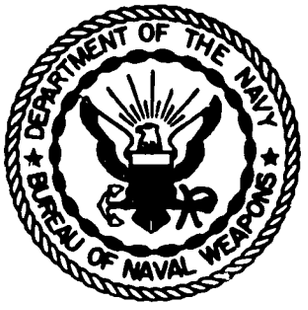

U. S. NAVAL WEAPONS LABORATORY
DAHLGREN, VIRGINIA

U. S. Naval Weapons Laboratory
Dahlgren, Virginia

Explosive Hardening of Iron and Low-Carbon Steel

by

L. A. Potteiger
Warhead and Terminal Ballistics Laboratory

NWL Report No. 1950

14 October 1964

CONTENTS

CONTENTS (Continued)

ABSTRACT

The degree and depth of shock hardening in iron and low-carbon steel plates was experimentally determined by detonating C-3 explosive against the plates. Final hardness levels were not strongly influenced by the magnitude of the pressure above the critical value of 130 kilobars or by explosive thickness or plate thickness, but were dependent upon the original hardness of the plate. The relative widths of the two hardness plateaus through the plate were found to depend upon explosive thickness, plate thickness, and applied pressure; a simple explanation for this dependence is presented in terms of the interaction of two shocks in the metal. The relationship of hardness and tensile strength was found to be about the same whether hardening was done explosively or by cold-working.

FOREWORD

This report covers one phase of an investigation of explosively induced stress waves in metals. This work was supported in part by Task Assignment 508-925/53025/04059 and in part by NWL Foundational Research Project 12014.

The author would like to acknowledge in particular the contribution of Mr. J. P. Rucker and Mr. V. E. Mason in the preparation of the many metallographic samples and the innumerable hardness measurements.

This report is based on a series of tests conducted by D. D. Abernathy, F. D. Altman, J. W. Hagemeyer, L. A. Potteiger and W. Sturges, III; and was reviewed by:

W. N. WISHARD, Head, Physics Branch, Research Division
J. C. TALLEY, Head, Research Division
W. E. McKENZIE, Assistant Director
R. I. ROSSBACHER, Director, Warhead and Terminal Ballistics Laboratory

APPROVED FOR RELEASE:

/s/ BERNARD SMITH
Technical Director

INTRODUCTION

This report presents data obtained from examination of slabs of iron and low-carbon steel which had been subjected to the direct force of a detonating high explosive in several simple geometrical arrangements. The data are discussed and several general principles are deduced from them which are thought to be of practical value. They are also interpreted qualitatively in terms of shock wave theory.

The general purpose of this series of experiments was to obtain data, useful for the design and development of explosive devices, concerning shock wave interaction in explosive-metal systems. In particular it was believed that interpretation of observed physical alteration in recovered metal pieces could be used to study the effect of variables in the explosive system. In addition this technique was expected to yield useful information on explosive-induced effects in the metals themselves.

Progress has been, and is being made on these objectives and this report is one of a series. In an earlier report of the series (reference 8) the works of Cyril Stanley Smith, reference 1, and Smith and Fowler, reference 7, were extended from the case of a normal shock to an oblique shock and the peak pressure induced in iron and low-carbon steel determined for several military explosives. Another report to be published, reference 9, will deal with spalling in iron and low-carbon steel. The present report covers a particular segment of the work and presents data thought to be of some interest, both for practical application and in relation to shock wave theory. For the latter purpose, the data are of interest in the existence, propagation and effects of a double plastic shock in certain ferrous metals, at applied shock pressures between approximately 130 and 340 kilobars (references 1 through 8). This double-shock phenomenon and its effects are thought to have practical importance both currently and potentially, in the research and development of explosive devices.

Many, although not all, of the principles deduced from the data in this report might have been predicted as consequences of the double shock theory. The data presented serve as additional experimental verification of its applicability in an area in which there are few experimental data. This area is one of some practical interest because it simulates conditions known to exist in many explosive devices. In particular it covers the case of the explosive which is thick relative to the metal plate which it accelerates, the case of both oblique and normal wave loading and the case of low-carbon steel as well as pure iron.

THEORETICAL BACKGROUND

The work described in this report is perhaps most directly related to that of Smith, reference 1, and Smith and Fowler, reference 7. Since these articles, supplemented by references listed in their bibliography, cover the theory of formation of the double shock wave quite thoroughly, the theory will be repeated here only in abbreviated and mostly qualitative form.

Bancroft, Peterson and Minshall (reference 6) have shown the existence of a double plastic shock in iron and have associated it with the discontinuity which occurs in the Hugoniot equation of state curve for iron at a pressure of approximately 130 kilobars. This double shock will be formed only if the induced pressure is within the range from 130 to about 340 kilobars (see Figure 14). Appendix A is a further discussion of the double shock region. (The relatively low-energy elastic wave arising from the structural characteristics of the metal is neglected here since it produces no permanent change.) In the double shock range there will be one shock traveling at a constant velocity, characteristic of the 130 kilobar critical pressure, given by

$$U_1 = V_o \left(\frac{P_c - P_o}{V_o - V_c} \right)^{1/2}$$

and a second shock traveling at a pressure-dependent velocity given by

$$U_2 = V_c \left(\frac{P - P_c}{V_c - V} \right)^{1/2} + U_{pc}$$

where $U_{pc} = \sqrt{(P_c - P_o)(V_o - V_c)}$ is the particle velocity. In all of these expressions P and V refer to pressure and specific volume, respectively, the subscripts o refer to original values, and the subscripts c to values at the point of inflection, or critical point, of the Hugoniot curve. All velocities are considered in terms of a stationary frame of reference. The second shock advances into material moving at the constant particle velocity U_{pc} given by the above expression. The second shock will lag behind the first shock unless the total pressure driving the second shock exceeds about 340 kilobars (see Appendix A); if the pressure is greater than

340 kilobars at the explosive-metal interface only a single shock will be formed, although this shock might later separate into a double-shock system as the pressure drops because of attenuation in passage through the plate. The condition for stability of the single shock is derived easily from the equations above. The pressure of 340 kilobars, required for a single shock, may also be obtained graphically from the Hugoniot curve for iron. It is seen to be the point of intersection, with the Hugoniot curve, of a straight line drawn from V_o through V_c, the critical point at 130 kilobars (see Figure 14).

Because of their different velocities the two shock fronts will become separated by a distance that depends, among other things, upon the distance traversed from the explosive-metal interface at which they originate. In the double-shock pressure range, therefore, the metal will be subjected first to a 130 kilobar shock and subsequently to a higher pressure shock.

The experimentally observed effect upon the hardness of certain ferrous metals of this passage of the two shock waves is shown in Figure 1. This figure shows the general features of a typical hardness traverse through a metal specimen which has had an explosive detonated in contact with one face, the opposite face being free to move. When the explosive-metal system is such that this occurs, it is found that two levels of hardening are preserved in the metal, with a more or less abrupt transition between them. The material in zone "A", which is nearest the explosive, is the hardest and this is the region which, according to the theory, has been subjected to a pressure exceeding 130 kilobars. The material in zone "B", which is the remainder of the plate, has been subjected to a pressure of just 130 kilobars, and has been hardened to a value intermediate between the original metal hardness and that of zone "A". Typical microstructure in the two zones is shown in Figures 2A and 2B.

The preservation of the two hardness zones in the recovered specimens, using the system referred to above, is a consequence of the transmission, reflection, and interaction of the two shocks in the metal. Smith's work (reference 1) shows how this process occurs and suggests that it might be used for the measurement of peak applied pressure. He notes some discrepancy, however, between his values determined by this method and by other experimental means. In a later paper, (reference 7) he and Fowler note a discrepancy in the pressure estimates used in the original paper. Upon correction and

further experiment the data are found to agree quite well with the theory (reference 7). Soper and Potteiger have derived a similar method to determine the peak applied pressure for an oblique detonation front (reference 8). Their results, using the data contained in this report along with data for other explosives, agree quite well with other published data.

The following explanation of the two hardness plateaus is essentially that presented in reference 1. It should be remembered that it applies only to pulses of long duration compared to the shock wave traversal time in the plates and hence does not apply to all of the data presented herein. Briefly the description is as follows: in the double-shock pressure range, the faster of the two shocks, which travels at a constant velocity characteristic of the 130 kilobar pressure, will reach the free surface of the metal ahead of the second shock which moves at a slower velocity dependent upon pressure. The fast 130 kilobar shock hardens the metal as it passes, but not as much as does the slower second shock. Upon reaching the free surface, the fast shock is reflected as a wave of rarefaction which then meets the oncoming second shock. The point of meeting is the point of transition between the two zones of hardness, "A" and "B" because it is here that the wave of rarefaction drops the pressure in the second shock wave below the greater-than-130-kilobar critical pressure which causes the extreme hardening of zone "A". Of course if the magnitude of the pressure of the second shock is greater than approximately twice the critical pressure of about 130 kilobars, its pressure would remain above the critical value after collision with the reflected rarefaction wave. In any case in the double shock region the pressure seen by zone "B" would be about 130 kilobars less than that seen by zone "A" or any part thereof. In general the data presented here are for cases where the magnitude of the second shock was reduced below 130 kilobars at the time of interaction. Although the magnitude of the second shock may be quite high initially as the shock enters the metal plate, it is attenuated by the work it does in hardening the plate and by the faster moving relief wave following the shock front; this attenuation will insure a drop below the critical pressure shortly after rarefaction wave collision even in the case described above.

The position of the transition between the two zones, as data presented herein will show, depends upon a number of factors in the explosive-metal system. A part of this dependence is described adequately by the above mechanism, but for shorter duration pulses a somewhat different but related mechanism is required; this will be described later under Results and Discussion.

EXPERIMENTAL METHOD

The principal factors covered by the results of these experiments are thickness, material and condition of the plate, thickness of the explosive charge and explosive pressure as affected by method of initiation. Measurements made before firing and variations of parameters employed in the test are discussed immediately following under the headings of Plate Description and Explosive System Description. Procedures used in firing and in after-firing analysis are discussed under the heading of Recovery and Analysis.

Plate Description

Low-carbon steel was used in the initial investigation of explosive-harding because some information was available on its impact hardening properties and it was expected to give clearly defined hardened zones. A limited number of the tests with steel were repeated with Armco iron to correlate this work with that of other investigators. A range of plate thicknesses from .1 to 0.95 inches was covered in ten steps. Table 1 contains a description of the material used for each sample thickness. All stock from which these samples were cut was received in the hot rolled, pickled and oiled condition. After machining to the test sample size, most of the plates were annealed in a vacuum furnace to a uniformly soft condition. A few plates were fired without annealing to evaluate the effect of a higher original hardness.

Representative samples were cut from the low-carbon steel and Armco stock and a series of before-firing hardness measurements made by a technique to be described later. Similar hardness traverses were made on the stock after annealing also. Hardness values in DPH obtained across the sample were then averaged and these are tabulated in Table 1. Figure 12 is representative of the pattern of hardness through the plate obtained from the unannealed and annealed low-carbon steel and the annealed Armco iron (unannealed Armco iron was not used in any of the rounds). Only minor differences from sample to sample are noted between the various steels; however, two samples of Armco stock showed an appreciable difference of twelve points DPH even though the chemical composition of the bars was found to be nearly the same, Figure 12.

Explosive System

The plastic explosive Composition C-3 was used for all the tests described in this report. It was hand packed into wooden rectangular forms of the appropriate sizes. Loading densities ranged from 1.5 to

1.6 grams per cubic centimeter. Explosive thicknesses ranged from .25 to 2.0 inches. The slab length and width were determined by the size of the test plate and the slab thickness. The explosive extended out beyond all edges of the test plate. This was done to reduce explosive edge effects.

Both line-wave (oblique) and plane-wave (normal) initiation of the explosive slabs were used. By so doing, it was possible to obtain significantly different applied pressures from the same thickness of explosive slabs.

In the line-wave technique, initiation took place essentially along one edge of the slab. This was accomplished either by an explosive lens system or simultaneous multiple point initiation as illustrated in Figure 4A. The detonation wave assumed a reasonably linear form (provided sufficient lead-in was allowed) as it swept across the slab, inducing an oblique stress wave in the metal plate. It was found (reference 8) that with C-3 explosive under these conditions the induced stress pulse has a peak pressure at the explosive-metal interface of approximately 170 kilobars. This pressure was independent of explosive thickness and plate mass, but these factors had a direct effect upon pulse length (duration).

The plane-wave initiation was effected through an adaptation of the duPont line-wave generator using EL-506-A sheet explosive. This system is shown in Figure 4B and is fully described in duPont Bulletin No. ES-58-2a. The glass driver plate initiated the Composition C-3 explosive directly so that use of sheet explosive as a receptor was not necessary. By making use of this system rather than a plane-wave lens system using two explosives, it was possible to generate a very short loading pulse of high intensity. The peak pressure induced in mild steel samples by this method of initiation was calculated to be at least 296 Kb (see Appendix A). The pressure duration was again determined by explosive and plate thickness although for a given set of conditions it was less than that for line wave initiation. The peak pressure was unaffected by explosive and plate thickness.

Plate Recovery and Analysis

The explosive slabs, with metal plates in intimate contact with the bottom face, were detonated on top of cardboard boxes filled with loosely packed sawdust, standing on several inches of celotex. Approximately four feet of sawdust and several inches of celotex were sufficient to stop most of the plates. Complete recovery of the metal plates or plate fragments was usually attained. The

recovered plates showed no evidence of damage caused by the recovery medium which would mask the effects caused by explosive loading. Figure 5 pictures a typical field set-up of a line-wave round prior to firing and Figure 6 shows the condition of two typical plates after firing.

After recovery the plates were sectioned and a sample was mounted, polished, and etched with a Nital solution. The sample was normally cut from the half of the plate opposite the detonation end (line-wave initiation only) and as near the width center-line of the plate as possible. By taking the samples at this location, plate edge effects were avoided. The variation in hardness along a line across the thickness dimension of the plate was determined for approximately one-fourth of the plates fired. Hardness measurements were not made on the remaining plates since the main interest was in the depth of the extreme hardened region. This depth was obtained quickly and easily by visual examination of the etched sample with a traveling microscope comparator. Figure 7 pictures plate A-4 (unannealed 0.5 low-carbon steel versus 0.997 C-3 explosive, line-wave) as etched. The decided change in appearance at what has been found to be the end of the extreme hardened region and beginning of the softer region can be seen quite easily.

The hardness measurements were made with a Kentron micro-hardness tester using a Vickers diamond pyramid 136 degree indenter. Indentations were usually made sixteen-thousandths of an inch apart in a straight line across the sample between the explosive loaded and free surfaces using a five-hundred gram load; the diagonals were then measured with a 50X objective. A typical line of hardness indentations may be seen across the center of the sample in Figure 7.

The tensile strength of two plates, after they had been hardened by explosive loading, was measured using square tensile specimens which were 3/16" x 3/16" x 5" in size. These specimens were cut to have uniform hardness in the test area. Four specimens were cut from the extreme hardened zone ("A") and four from the intermediate zone ("B"). Two of each four were cut from a plate that had been annealed before firing and two from a plate that had not. Both Rockwell B and Diamond Pyramid Hardness (DPH) measurements were made in each zone.

RESULTS AND DISCUSSION

The principal results and test variables for all of the tests reported herein may be found in Tables 2 and 4. Additional detailed results for certain of these tests and various summaries of the data may be found in the Tables and Figures.

The results are discussed under three main headings as follows: (1) Depth of Extreme Hardened Region, (2) Increase of Hardness Level, and (3) The Relationship of Hardness and Tensile Strength of Explosively-Hardened Metal.

Depth of the Extreme Hardened Region

a. Effect of Obliquity of Detonation Front

The depth of extreme hardening data in Table 3 and plots of hardness versus distance from the free surface in Figures 8, 9, and 10 indicate clearly that there is a much greater depth of extreme hardening for a plane-wave (normal) shock than for a line-wave (oblique) shock if other conditions remain unchanged. In all cases the normal shock was produced by the method of plane-wave initiation, Figure 4b, and the oblique shock by the method of line-wave initiation, Figure 4a, which were described earlier. There are also in Table 3 several comparisons between the depth of hardening in Armco iron and low-carbon steel among the data for the 0.35 plates. The depth of hardening in the iron appears to be somewhat less than in the steel. The differences, although consistent, may be insignificant.

The amount of increase in depth of extreme hardness region in going from oblique to normal shock is seen (in Table 3) to vary considerably with both plate thickness and explosive thickness. This increase in depth of the extreme-hardened zone is believed to be controlled principally by the incident pressure for the following reasons: The amount of explosive used in the two cases is virtually the same, hence there should be no significant change in total applied impulse. With a change from line-wave to plane-wave initiation there is known to be an increase in peak pressure and a decrease in duration of pressure at the explosive-metal interface. For an applied impulse of long duration, relative to the shock traversal time in the plate, an increase in pressure is known to increase the depth of hardening, and as suggested earlier, may even be used to measure peak pressure (see references 1 and 7 and Appendix A). As will be seen from results presented below, a decrease in duration of pressure can only reduce the depth of hardening. In summary then, there are two competing effects caused by a change from line-wave to plane-wave initiation: an increase in depth of extreme hardening caused by an increase in peak pressure, and a decrease in depth of hardening caused by a decrease in pressure duration Of these two the peak pressure is evidently the controlling factor, since the depth increases in every instance with an increase in peak pressure

even with pulses of decreased duration. The large variability shown is evidently the result of the competing effects, although a simple relationship has not yet been found which would permit prediction of the amount of increase.

b. Effect of Explosive Thickness

The depth of extreme hardening is also dependent on the thickness of high explosive used but only up to a certain thickness, after which the depth becomes a constant dependent only on the plate thickness (and the pressure as stated above). This is illustrated by Figure 11, which shows the hardened zone (zone "A") thickness plotted against explosive thickness for the line-wave experiments. The plane-wave data were not plotted because of the small number of data points. These results are explained in the following paragraph.

If the explosive thickness is small relative to that of the plate, the duration of the pressure pulse will be short relative to the time required for the first, or 130 kilobar, shock in the metal to traverse the plate and be reflected from its free surface. This shortness of the pressure pulse allows the peak pressure in the second shock to drop below 130 kilobars before meeting the reflected first shock. The point at which the pressure in the second shock drops below 130 kilobars, whatever the reason, marks the end of the zone of extreme hardening. It is evident that the point at which this occurs will be later, and hence the extreme-hardened zone thicker, as explosive thickness is increased. A point will be reached eventually, however, where the explosive is thick enough and the pressure pulse long enough, to maintain the pressure pulse in the second shock reasonably constant, above 130 kilobars, until it meets the reflection from the first shock. Any further increase in explosive thickness beyond this critical thickness, unless accompanied by a different peak pressure, will not change the point at which collision takes place and hence will not change the depth of hardening.

It is evident from Figure 11 that this explanation fits the experimental data. For several plate thicknesses there is a curve showing the increase of extreme-hardened zone thickness with increase of explosive thickness; in the case of at least three plate thicknesses a value has been reached which remains constant with further increase in explosive thickness. In the case of the thicker plates, a constant value has not yet been demonstrated, but it seems probable that with still thicker layers of explosive it will be.

c. Effect of Original Plate Hardness

The data plotted in Figure 11 were examined to see whether the original hardness of the plate had any effect on the depth of extreme-hardening. Since these data did not include test samples in which there were large differences in original hardness, the change in depth of hardening was masked to some extent by normal experimental scatter. Out of nine shots, in which conditions other than original hardness were the same, there were only three in which the depth of extreme-hardening was less for an unannealed, than for an annealed steel plate. The difference in original hardness of annealed and unannealed steel plates ranged from 14 to 17 points DPH which was apparently insignificant.

Increase of Hardness Level

a. Effect of Obliquity of Detonation Front

The increase in hardness levels, as distinguished from depth of extreme-hardening, does not appear to be a strong function of the method of initiation of the explosive, and hence not of the peak pressure applied at the metal surface. Since detailed hardness measurements were not made on every sample, there are fewer direct comparisons on this question than on the depth of hardening; however, Figures 8, 9 and 10 show that in all four cases, which were selected for complete hardness traverses, the hardness in both regions is about the same whether line-wave or plane-wave initiation was used. As mentioned earlier there is an appreciable difference in peak applied pressure for the two initiation methods. A still greater pressure difference, which could be obtained by use of other explosives, might produce a hardness difference large enough to show up in the presence of normal experimental scatter; however, the use of line-wave and plane-wave initiation with C-3 explosive produces pressures which are within the range of pressures of interest in many current explosive applications. In these current applications, therefore, the increase in hardness level (but not depth) as a function of method of initiation, or of position of the metal relative to the point of initiation, is not thought to be a factor of importance. Dieter has shown, reference 7, a great increase in the hardness level of iron with increasing pressure up to about 200 Kb after which an increase in pressure does not appear to affect the final hardness level.

The curve of hardness vs distance for plate E-6 in Figure 10B presents a rather unusual appearance, which thus far has not been explained satisfactorily. In this curve there is a rather marked drop in hardness at the explosive surface which persists for a

considerable distance into the plate. Drops in hardness near the explosive surface have been observed rather often in other plates but not nearly to this depth or extent. There did not appear to be any micro-fissures to cause the decrease in hardness level.

b. Effect of Explosive Thickness

There appears to be a very slight but noticeable increase in hardness level as explosive thickness is increased. This increase occurs in both the extreme-hardened zone ("A") and the intermediate zone ("B") by approximately the same amounts. Attenuation of the pressure pulse as it traverses the plate may be the reason for this. With a thicker explosive, the duration of the pressure pulse is increased, thereby slowing the rate of attenuation. The amount of increase is only about eight points DPH, with an increase in explosive thickness from 1/4 inch to two inches, and hence is not thought to be an important factor even for rather large thicknesses of explosive.

c. Effect of Original Plate Hardness

The plate hardness before firing influences the final hardness value in the two zones, but the number of points hardness increase above the original value is approximately constant for each zone. This is shown by the data of Table 2, is presented graphically in Figure 13, and summarized below:

AVERAGE HARDNESS IN DPH

	Annealed Iron	Annealed Steel	Unannealed Steel
Original	92	117	131
Zone A	211	235	247
Zone B	147	170	189
Zone A minus Original	119	118	116
Zone B minus Original	55	53	58

In Figure 13 the plates were grouped according to original hardness. A considerable amount of scatter is present in the after-firing hardnesses. However, by comparing the average values for the three groups, it is evident that higher original hardness leads to higher final hardness in both zone "A" and zone "B".

It is interesting to note that the amount of increase in hardness in each zone appears to be independent of original hardness. It must be emphasized, however, that the range of original hardnesses considered here is quite small and at the soft end of the hardness spectrum. No information is available on the explosive hardening of iron and low-carbon steel plates of high original hardness. Other materials tested appear to exhibit a saturation hardness level, i.e., the softer the material before explosive loading the greater the increase in hardness level and vice versa. Very hard materials work harden only slightly as a result of explosive loading, reference 11.

The Relationship of Hardness and Tensile Strength of Explosively-Hardened Metal

There is little if any difference in the hardness values associated with a given tensile strength, whether the hardening was done explosively or by cold-working. This may be seen in Table 5. The table shows values of measured tensile strength, elongation and reduction of area for four samples taken from the extreme-hardened zone ("A") and four from the intermediate hardened zone ("B"). The specimens designated B-8 were annealed before-firing; those designated U were not. The measured sample hardnesses in both Rockwell B and DPH scales are tabulated for each test. Typical hardness values for cold-worked steel of similar composition which should give the same tensile strengths were obtained as noted on Table 5. Comparison of the measured hardness values for explosive-hardening with these hardness values for cold-worked metal of equal tensile strength show no significant difference between the two.

Thus it appears that in low-carbon steel there is no significant difference in tensile properties for equal hardness, whether hardening was done explosively or by cold-working.

CONCLUSIONS

For solid iron and low-carbon steel plates, originally soft and hardened by the detonation of Composition C-3 high explosive in direct contact, it is concluded that:

1. The degree (as opposed to extent) of hardening is affected only slightly, if at all, by the following factors:

   a. explosive thickness

   b. plate thickness

   c. variations in the applied pressure in the pressure range of these tests

2. An increase in the original hardness of the metal appears to increase the residual hardness as a result of explosive action in all parts of the plate.

3. The variation in hardness, along a line normal to the explosive surface and through the plate, follows a double-plateau pattern, the characteristics of which are predictable in terms of explosive thickness, plate thickness and the applied pressure; this variation can be explained plausibly and simply in terms of the interaction of two shocks in the metal.

4. The relationship of hardness and tensile strength is approximately the same whether hardening was done by cold-working or by contact explosives.

REFERENCES

1. Smith, C. S., "Metallographic Studies of Metals After Explosive Shock", Trans. Metall. Society A.I.M.E., October 1958, p. 574
2. Katz, S. and R. E. Peterson, "Study of Shock Propagation in Ferrous Metals", Poulter Laboratories Technical Report 010-55, Stanford Research Institute, December 1955
3. Pearson, J. and J. S. Rinehart; "Hardness Plateaus and Twinning in Explosively Loaded Mild Steel", Journal of Applied Physics, Vol. 25, p. 778 (1954)
4. Singh, S., N. R. Krishnaswamy, and A. Soundraraj, "Hardness Plateaus and Twinning in Steel by Explosives with Lined Cavities", Journal of Applied Physics, Vol. 27, p. 617 (1956)
5. Rinehart, J. S., "Work Hardening of Mild Steel by Explosive Attack", Journal of Applied Physics, Vol. 22, p. 1086(L) (1951)
6. Bancroft, D. E., L. Peterson and S. Minshall, "Polymorphism of Iron at High Pressure", Journal of Applied Physics, Vol. 27, p. 291 (1956)
7. Smith, C. S., and C. M. Fowler, "Response of Metals to High Velocity Deformation" (Interscience Publishers, Inc., New York, 1961) p. 309
8. Soper, W. G. and L. A. Potteiger, "Explsive-Induced Pressures in Iron", NAVWEPS Report No. 7669 (Nov. 1961); also Journal of Applied Physics, 34, 1817 (1963)
9. Potteiger, L. A., "Spalling of Iron and Low Carbon Steel by Several Military Explosives", NAVWEPS Report No. , to be published (1965)
10. Dieter, G. E., Response of Metals to High Velocity Deformation (Interscience Publishers, Inc., New York, 1961) p. 409

REFERENCES (Continued)

11. Potteiger, L. A., "Explosive Hardening of Nickel Mar-Aging and Manganese Steels", USNWL Report No. 1934, 9 Sep 1964
12. Deal, W. E., "Measurement of the Reflected Shock Hugoniot and Isentrope for Explosive Reaction Products", Physics of Fluids, I, 523 (1958)
13. Minshall, F. Stanley, "Response of Metals to High Velocity Deformation" (Interscience Publishers, Inc., New York, 1961) p. 249
14. Walsh, J. M., M. H. Rice, R. G. McQueen, and F. L. Yarger, "Shock-Wave Compressions of Twenty-Seven Metals, Equations of State of Metals", Journal of Applied Physics, Vol. 108, p. 196, (1957)
15. McQueen, R. G., and S. P. Marsh, "Equation of State for Nineteen Metallic Elements from Shock-Wave Measurements to Two Megabars", Journal of Applied Physics, Vol. 31, p. 1253 (1960)
16. Soper, W. G. Private Communication

APPENDIX A

PLANE-WAVE PRESSURE CALCULATION

C. S. Smith, references 1 and 7, has shown that the location of the transition or interaction zone in an iron specimen can be used to determine the pressure applied by a normally incident detonation wave. W. G. Soper, reference 8, has extended Smith's technique to include loading by oblique detonation waves. In either case if a single test specimen is considered, the calculated pressure will be the pressure determined from the average velocity of the second, high pressure shock in the extreme-hardened zone, zone "A", of the specimen; this pressure is a fair approximation of the average peak pressure seen by zone "A" of the specimen. If however a sufficient number of data points are available for small ratios of plate thickness to explosive thickness, h/l, and the induced pressure is in the double shock region, the peak pressure induced in the metal at the explosive-metal interface may be calculated in addition to the average peak pressure in the region, see reference 8 and below.

The methods of Smith and Soper have been combined here to calculate a value for the peak pressure induced in iron and low-carbon steel by plane-wave detonation of Composition C-3 explosive in direct contact using the data contained in this report and additional data generated from similar tests to be described below. An alternate, but similar method using the pressures calculated by Smith's method to plot pressure attenuation curves was also used to determine this pressure. The pressure calculated by both methods is an approximation of the minimum peak pressure induced in the metal at the explosive-metal interface. Unfortunately the methods appear to be unsuitable for exact measurement of pressures near the upper limit of the double shock region, approximately 340 kilobars; the reasons for this are discussed below in some detail.

In Table A-1 data are tabulated for twenty-four plane-wave rounds. These data include the original and final plate thickness, the explosive thickness, depth of zone "A" both as measured and as corrected, the ratios of hardened zone thickness and plate thickness to explosive thickness, hardened zone thickness to plate thickness, and U_2, the velocity of the second shock to U_1, the velocity of the first, 131 kilobar shock, and pressure. The final plate thickness is the average thickness of the specimen plate after explosive loading; some residual compression of the plates due to lateral expansion is evident in most cases. The corrected depth of zone "A" is the product of the average measured depth of zone "A" and the ratio of original plate thickness to final plate thickness. The velocity ratio, U_2/U_1, was calculated using the equation given below, derived by Smith. The pressure was determined from Smith's curve, reference 7, relating pressure to U_2/U_1.

In Table A-2 additional data are tabulated for twelve different, but similar plane-wave rounds. In these tests the circular Armco iron specimen plates (4"0 diameter) were press-fitted into the center of larger, circular low-carbon steel plates (9"0 diameter) attached to one end of a low-carbon steel right-circular cylinder of length equal to the explosive thickness. The assemblies are described in NWL Drawing No. T-30102. The plastic explosive Composition C-3 was loaded in the cylinders and the end opposite the specimen plate was plane-wave initiated using the generator illustrated in Figure 4b, Appendix C. The steel specimen surround and steel explosive cylinder served to reduce specimen edge effects and increase, somewhat, the explosive pressure pulse duration. In all other respects these and the other tests with wood surrounds and explosive containers were similar; the results of the two tests are considered equal for the pressure determinations.

In Figure A-1 the ratio of zone "A" thickness to explosive thickness is plotted against the ratio of plate thickness to explosive thickness. Although the data are somewhat scattered, a definite pattern is evident. (See reference 8 for an explanation of the observed pattern.) The asymptote to the curve through the point 0,0 is important to the required calculation. Considering the data, three possible asymptotes are plotted; (1) the steepest corresponding to an a/h of 0.9956, plate J-11, (2) the average of the ten data points below h/1 = 0.3, a/h = 0.970, and (3) the average of the thirty-three data points below h/1 = 1.0 for which a/h = 0.906. The asymptote for a/h = 1 is also shown for comparison as explained below. Of these the value of 0.970 for a/h is considered the best fit.

Smith derived the following equation for the ratio of the velocities of the first and second shocks, see references 1 and 7:

$$U_2/U_1 = 1 - c_o/\rho_1 + \rho_o/\rho_1 \left[(1 - r)/1 + (U_1/c_o)r\right]$$

where

U_2 = velocity of the second shock

U_1 = velocity of the first, 131 kilobar shock

ρ_o = initial density at ambient pressure and temperature

ρ_1 = density under first shock conditions

ρ_o/ρ_1 = 0.936 for iron and low-carbon steel

r = ratio of soft zone, zone "B", thickness to plate thickness or one minus the ratio of hard zone, zone "A", thickness to plate thickness

c_o = sound speed = 4.70 mm/μsec. for rarefaction from 100 to 150 kb.

and

$$U_1/c_0 = 1.075 .$$

This equation was used with the values of a/h cited above to obtain U_2/U_1 values of 0.9915, 0.944, and 0.834 corresponding to values of r of 0.0044, 0.030, and 0.094, respectively. In reference 7, Smith has plotted U_2/U_1 versus pressure, a relationship determined from the Hugoniot curve for iron. The above values of U_2/U_1 give pressure values of 324, 296, and 241 kilobars, respectively. The value of 296 kilobars is considered best for the data presented; however, a better approximation could be made using this method if additional data points for lower values of h/1 were available. For reasons that will appear below, the value calculated is probably too low.

The limiting asymptote as h/1 approaches zero, Figure A-1, is the one for which a/h = 1, i.e., for which the extreme-hardened zone thickness equals the plate thickness. For a/h = 1 the pressure calculation fails since this implies a single shock. Thus if zone "B", the softer zone next to the free surface, is present in a recovered iron specimen after explosive shocking, a double shock system is inferred with a peak pressure between 131 and 340 kilobars. Smith, however, has detected zone "B" in iron specimens after loading at pressures above 340 kilobars to 450 kilobars, reference 7. The width of the zone was independent of pressure above 340 kilobars. He reports, reference 7, the presence of zone "B" after shock loading above 340 kilobars ".....may indicate some structure to the shock front or it may be evidence of the region of reverberating elastic wave discussed by Minshall", reference 13. Soper is of the opinion that above 340 kilobars the pressure pulse still has the appearance of a double shock (structure to the shock front), but its shape is constant with time, i.e., a finite yield time, or time for a phase change to take place, is required for peak pressures above 131 kb., (reference 16). A zone "B" of finite width has been detected in low-carbon steel specimens after plane-wave detonation of Composition B explosive in direct contact; the plates were relatively thin compared to the explosive thickness and the pressure pulse of long duration and magnitude greater than 340 kb. (see below) in these tests.

Soper, reference 8, calculated the peak pressure induced in iron by line-wave detonation of Composition C-3 in direct contact to be 170 kb and by Composition B to be 180 kb, almost an insignificant difference at these pressures. W. E. Deal, reference 12, determined the peak pressure to be 453 ± 2.6 kb induced in ordinary yellow brass by plane-wave detonation of Composition B in direct contact. The Hugoniot for iron is very nearly the same as that for brass, therefore the peak pressure induced in iron by plane-wave detonation of

Composition B in direct contact is roughly 450 kb. The value of 296 kb calculated here for plane-wave detonation of Composition C-3, therefore, appears to be too low. A value around 400 kb is considered more nearly correct. Minshall, reference 13, states "It is clear,....., that the pressure of the plastic I wave (131 kb) decreases slowly with distance, and that both the pressure and velocity of the plastic II wave (greater than 131 kb) decrease rapidly with distance." Thus, in light of all of the above, the pressure calculation here could be expected to yield a low value. If indeed the peak pressure induced in iron and low-carbon steel by plane-wave detonation of Composition C-3 explosive in direct contact is around 400 kilobars and for pressures above 340 kilobars, zone "B" is still formed, the peak pressure cannot be determined using the location of the interaction or transition zone to calculate U_2/U_1. To know when the calculation is appropriate, a wealth of data for very small h/l is required and/or an estimate of the peak pressure induced is required.

A similar, alternate method for determining the peak pressure induced at the explosive-metal interface is illustrated in Figure A-2. Here the pressures tabulated in Tables A-1 and A-2 are plotted versus plate thickness for the various explosive thicknesses to obtain a family of pressure attenuation curves, one for each thickness of explosive. All of these curves should cross the ordinate for zero plate thickness at the same value of pressure because only the explosive pressure pulse duration and not the peak pressure induced, is a function of the explosive thickness. This value of pressure is the peak pressure induced, in this case, in iron and low-carbon steel at the explosive-metal interface by plane-wave detonation of Composition C-3 explosive in direct contact.

In Figure A-2 the attenuation curves shown are linear. The shape of these curves should be in all probability concave upward by virtue of the shape of the induced pressure pulse and the shape of the Hugoniot cruve for iron, Figure 14, Appendix C. Minshall, reference 13, shows an attenuation curve for iron based on four data points with a concave upward shape. Because of scatter in the data only a least squares linear fit was used here.

Obviously the data for the one inch thickness of explosive are more scattered than that for the other thicknesses, perhaps because there are more data for the one inch. As noted on Figure A-2 three of these data points were excluded from the least squares fit. Considering this fit and the least squares linear fits to the other data, the average ordinate crossing occurs at a pressure value of approximately 316 kilobars; this value is plus or minus roughly 25 kilobars.

Most of the above discussion applies to this method of pressure determination also. It is obvious that unless a wealth of consistent data are available, the shape of the attenuation curves and therefore the peak pressure induced cannot be accurately determined. As noted previously a value of 296 or even 316 kilobars is considered too low for the peak pressure induced in iron and low-carbon steel by plane-wave detonation of Composition C-3 explosive in direct contact. A value around 400 kilobars is considered more nearly correct in light of all of the above.

TABLE A-1

DATA OF PLANE-WAVE ROUNDS FOR PRESSURE DETERMINATION

Plate Designation	Orig. Plate Thickness(h) (inch)	Final Plate Thickness(h') (inch)	Explosive Thickness(l) (inches)	Depth of Zone "A" (a') (inch)	Corrected Depth of Zone "A" (a) (inch)	a/l	h/l	a/h	U_2/U_1	Pressure (kilobars)
2C-12	0.198	0.181	0.500	0.169	0.185	0.370	0.397	0.934	0.880	263
*2D-12	0.450	0.439	0.500	0.289	0.298	0.596	0.700	0.852	0.752	203
2E-12	0.451	0.438	0.500	0.300	0.312	0.624	0.702	0.888	0.806	228
Y-4	0.936	0.910	0.500	0.326	0.335	0.670	1.872	0.358	0.262	---
K-14	0.450	0.451	0.747	0.404	0.403	0.540	0.602	0.896	0.818	234
J-14	0.956	0.906	0.747	0.594	0.627	0.839	1.280	0.656	0.512	135
1C-12	0.198	0.192	1.026	0.179	0.185	0.180	0.193	0.932	0.879	262
*1D-12	0.450	0.407	1.026	0.280	0.319	0.311	0.341	0.912	0.844	246
1E-12	0.351	0.322	1.026	0.308	0.336	0.328	0.342	0.956	0.918	282
E-6	0.351	0.340	1.029	0.307	0.317	0.308	0.341	0.903	0.829	239
K-15	0.450	0.391	1.009	0.320	0.368	0.365	0.446	0.818	0.704	180
K-7	0.486	0.466	1.016	0.320	0.334	0.329	0.478	0.687	0.545	137
P-9	0.552	0.505	1.009	0.358	0.391	0.388	0.547	0.709	0.569	139
O-2	0.650	0.618	1.005	0.554	0.583	0.580	0.647	0.896	0.818	234
N-2	0.750	0.721	1.007	0.620	0.645	0.641	0.745	0.860	0.764	208.5
R-5	0.851	0.806	0.997	0.649	0.685	0.687	0.854	0.805	0.689	173
X-4	0.936	0.822	1.026	0.687	0.782	0.762	0.912	0.836	0.729	192
J-6	0.957	0.919	1.029	0.780	0.812	0.789	0.930	0.849	0.748	201
J-9	0.955	0.888	1.016	0.730	0.785	0.773	0.940	0.822	0.710	183
B-7	0.355	0.332	1.507	0.319	0.341	0.226	0.236	0.961	0.927	286.5
K-6	0.486	0.462	1.516	0.444	0.467	0.308	0.321	0.961	0.927	286.5
P-10	0.552	0.533	1.515	0.494	0.512	0.338	0.364	0.927	0.868	257
N 11	0.751	0.730	1.514	0.669	0.688	0.454	0.496	0.916	0.850	248.5
J-10	0.956	0.876	1.516	0.814	0.889	0.586	0.631	0.929	0.872	259

*Armco iron plates

TABLE A 2

DATA OF ADDITIONAL PLANE-WAVE ROUNDS FOR PRESSURE DETERMINATION

Plate* Designation	Orig. Plate Thickness(h) (inches)	Final Plate Thickness(h') (inches)	Explosive Thickness(l) (inches)	Depth of Zone "A" (a')(inches)	Corrected Depth of Zone "A" (a)(inches)	a/l	h/l	a/h	U_2/U_1	Pressure (kilobars)
E-8	0.250	0.225	1.50	0.217	0.241	0.161	0.167	0.964	0.933	290
D-7	0.500	0.485	1.50	0.457	0.471	0.314	0.333	0.942	0.894	270
M-14	0.625	0.599	1.50	0.564	0.588	0.392	0.417	0.942	0.894	270
N-15	2.000	1.946	1.50	~ 1.046	1.075	0.717	1.333	0.538	0.400	132
C-5	0.250	0.242	3.00	0.240	0.248	0.0827	0.083	0.992	0.985	320
A-1	0.500	0.489	3.00	0.480	0.491	0.1637	0.167	0.982	0.966	308
A-3	0.500	0.476	3.00	0.468	0.492	0.164	0.167	0.983	0.968	310
B-4	1.000	0.980	3.00	0.933	0.952	0.317	0.333	0.952	0.911	278.5
K-12	0.375	0.341	6.00	0.331	0.364	0.061	0.0625	0.971	0.945	296.5
J-11	0.500	0.456	6.00	0.454	0.498	0.083	0.083	0.9956	0.9915	324
L-13	0.625	0.574	6.00	0.550	0.599	0.0998	0.104	0.958	0.922	284
H-10	1.000	0.924	6.00	0.886	0.959	0.1598	0.167	0.959	0.924	285

*All plates were Armco Iron

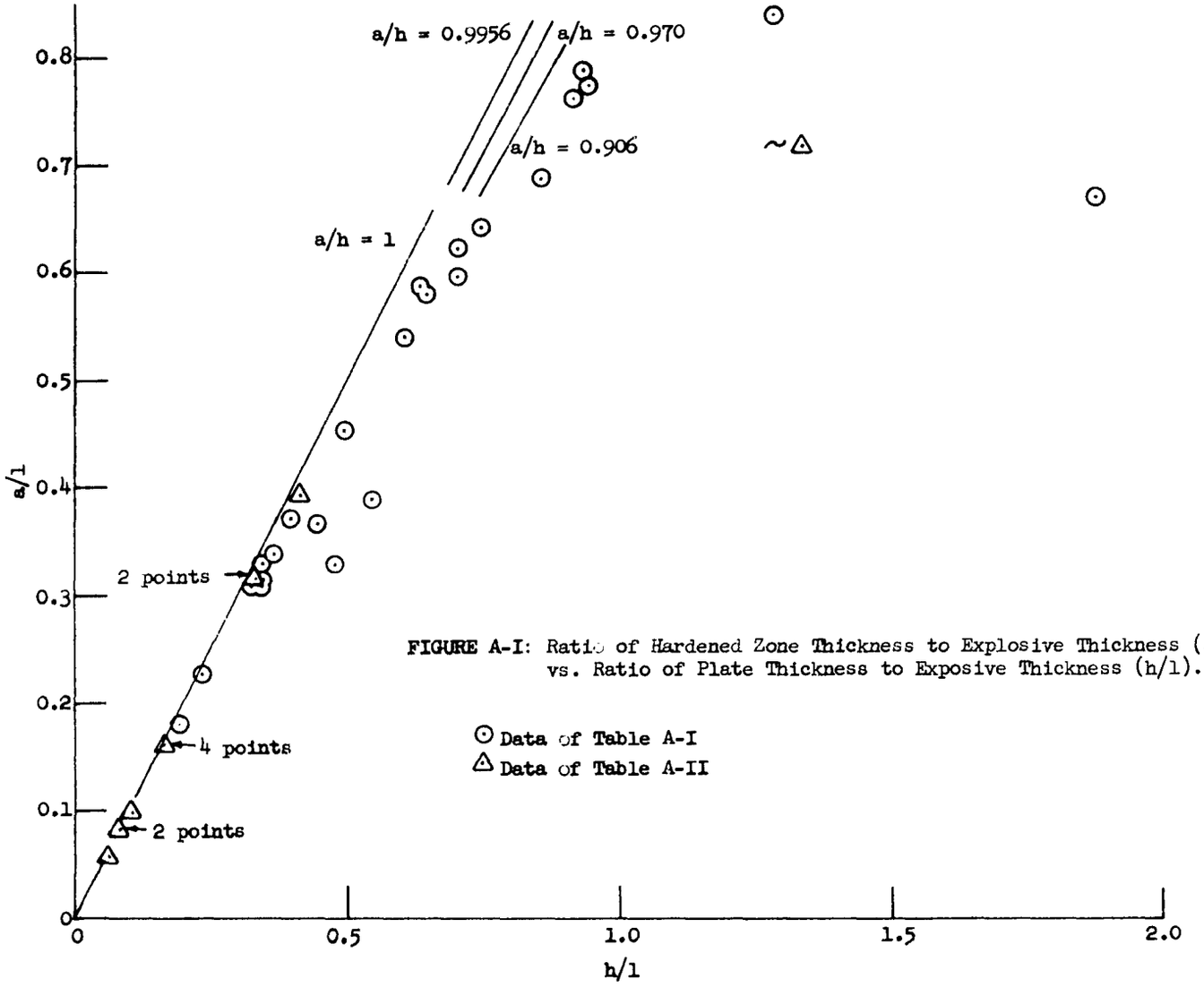

FIGURE A-I: Ratio of Hardened Zone Thickness to Explosive Thickness (a/l) vs. Ratio of Plate Thickness to Exposive Thickness (h/l).

⊙ Data of Table A-I
△ Data of Table A-II

Figure A-2: Calculated Pressure Vs. Plate Thickness for Plane-Wave Initiation of Composition C-3 Explosive and Mild Steel/Armco Iron Plates in direct contact.

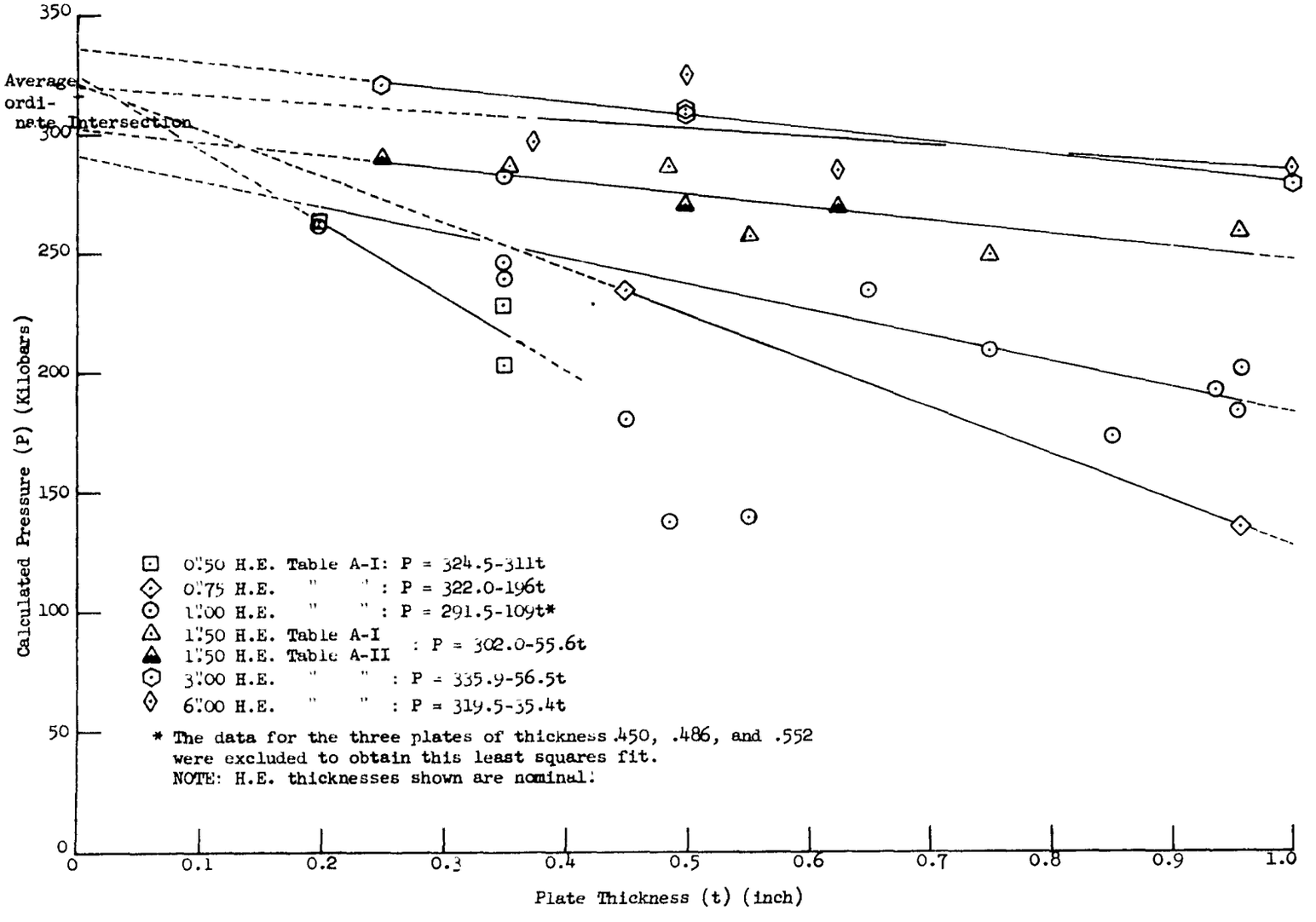

APPENDIX B

TABLE 1 DIMENSIONS AND CHARACTERISTICS OF THE TEST PLATES

STEEL

Nominal Thickness (inch)	Test Sample Dimension* (inches)	Carbon %	AISI Grade Designation	Diamond Pyramid Hardness** Annealed Plate	Diamond Pyramid Hardness** Unannealed Plate
0.1	3 x 6	0.177	1016	114	***
0.2	3 x 6	0.177	1016	114	132
0.35	3 x 6	0.236	1025	117.8	131.4
0.45	3 x 6	0.236	1025	117.8	131.4
0.5	3 x 6	0.236	1025	117.8	131.4
0.55	3 x 6	0.162	1015	107.7	***
0.65	3 x 6	0.184	1022	108.7	***
0.75	5 x 6	0.211	1022	115.4	***
0.85	5 x 6	0.160	1015	119.7	***
0.95	5 x 6	0.211	1022	115.4	***
0.95	6 x 6	0.188	1022	115.4	132.2

ARMCO IRON 99.8% PURE

Nominal Thickness (inch)	Test Sample Dimension* (inches)	Diamond Pyramid Hardness** Annealed Plate
0.1	3 x 6	79.5
0.2	3 x 6	79.5
0.3	3 x 6	92
0.35	3 x 6	92

*All plates were cut with the 6 inch dimension along the direction of rolling of the bar stock.

**These are average hardnesses taken before firing (DPH, 500 gram load). Several hardness traverses through unloaded plates are plotted in Figure 12.

***None of these plates were explosively loaded so hardness was not measured.

TABLE 2

HARDNESS VALUES AND DEPTH OF ZONES "A" AND "B" FOR LOW-CARBON STEEL AND ARMCO IRON

Plate Designation	Original Plate Thickness (inch)	Explosive (C-3) Thickness (inches)	Average DPH(1) Value Before Firing	Average DPH(1) Value After Firing Zone "B"	Average DPH(1) Value After Firing Zone "A"	Depth of*** Zone "A" (inch)	Depth of*** Zone "B" (inch)
			Annealed Armco Iron				
D-4	0.350	0.988	92	155	217	0.234	0.100
1D-12*	0.350	1.026	92	139	206	0.280	0.027
		Average Values	92	147	211.5		
			Annealed Low-Carbon Steel				
Q	0.936	0.257	115	174	265**	0.140	0.795
K	0.458	0.497	118	155	231**	0.143	0.310
A-9	0.936	0.499	115	176	260	0.196	0.740
E-9	0.352	1.003	118	172	228	0.227	0.112
E-6*	0.351	1.029	118	160	215	0.307	0.033
A-7	0.458	1.040	118	180	239	0.294	0.146
N-1	0.749	1.018	115	167	226**	0.310	0.428
N-2*	0.750	1.007	115	166	240	0.620	0.101
A-8	0.458	1.496	118	175	234	0.248	0.170
K-2	0.486	1.501	118	160	218	0.290	0.175
K-6*	0.486	1.516	118	161	221	0.444	0.018
B-8	0.936	1.501	115	188	245	0.512	0.394
K-4	0.486	2.013	118	169	228	0.267	0.168
J-11	0.956	2.052	115	181	234	0.593	0.301
		Average Values	117	170	234.6		
			Unannealed Low-Carbon Steel				
A-2	0.216	0.242	132	192	244	0.074	0.142
1	0.462	0.250	131	186	225**	0.089	0.370
0	0.939	0.256	132	182	255**	0.144	0.795
S	0.465	0.366	131	194	241	0.152	0.297
A-1	0.215	0.512	132	189	252	0.121	0.093
D	0.462	0.508	131	187	238	0.198	0.242
G	0.460	0.629	131	186	236	0.244	0.204
A-5	0.197	0.741	132	200	279	0.134	0.076

TABLE 2 (Continued)

Plate Designation	Original Plate Thickness (inch)	Explosive (C-3) Thickness (inches)	Average DPH(1) Value			Depth of***	
			Before Firing	After Firing		Zone "A" (inch)	Zone "B" (inch)
				Zone "B"	Zone "A"		
			Unannealed Low-Carbon Steel (Continued)				
J	0.456	0.740	131	189	234	0.255	0.186
T	0.939	0.738	132	178	246	0.314	0.624
A-6	0.197	1.010	132	196	264	0.145	0.046
A-4	0.456	0.997	131	200	255	0.292	0.143
U	0.936	0.972	132	179	237	0.415	0.475
		Average Values	131.5	189	246.6		

(1)Diamond Pyramid Hardness, 500 gram load, 50X objective.

*Plane-Wave Initiation.

**The maximum value of hardness reached in Zone "A" - the degree of hardening is not constant.

***The depth, or thickness, of both zones does not add to the original plate thickness due to residual compression of the specimen after explosive loading.

TABLE 3

EFFECT OF OBLIQUITY OF DETONATION FRONT ON DEPTH OF HARDENING

Nominal** Plate Thickness (inch)	Nominal** Explosive Thickness (inch)	Average*** Thickness of Zone "A"	
		Oblique Shock (inch)	Plane-Wave Shock (inch)
0.20	0.5	0.121 (1)	0.169 (1)
0.20	1.0	0.145 (1)	0.179 (1)
0.35	0.5	0.177 (1)	0.300 (1)
0.35*	0.5	0.171 (1)	0.289 (1)
0.35	1.0	0.248 (2)	0.308 (2)
0.35*	1.0	0.234 (1)	0.280 (1)
0.35	1.5	0.227 (3)	0.319 (1)
0.45	0.75	0.255 (1)	0.404 (1)
0.45	1.0	0.293 (2)	0.320 (1)
0.50	1.5	0.290 (1)	0.499 (1)
0.55	1.0	0.304 (1)	0.358 (1)
0.55	1.5	0.364 (1)	0.495 (1)
0.65	1.0	0.288 (1)	0.554 (1)
0.75	1.0	0.339 (1)	0.605 (1)
0.75	1.5	0.422 (1)	0.669 (1)
0.85	1.0	0.420 (1)	0.649 (1)
0.95	0.5	0.217 (2)	0.326 (1)
0.95	0.75	0.314 (1)	0.594 (1)
0.95	1.0	0.421 (2)	0.732 (3)
0.95	1.5	0.540 (2)	0.814 (1)

*Armco test plates - all others are low-carbon steel.

**Both the actual plate thickness and explosive thickness were within 3% of the nominal thicknesses listed.

***Average values based on the number of tests shown in parenthesis. No correction factor has been used to compensate for differences in explosive thickness or original plate thickness or final compressed plate thickness.

TABLE 4

DEPTH OF ZONES "A" AND "B" FOR LOW-CARBON STEEL AND ARMCO IRON

Plate Designation	Original Plate Thickness (inch)	C-3 Explosive Thickness (inches)	**Depth of Zone "A" (inch)	**Depth of Zone "B" (inch)
		Annealed Armco Iron		
G-1	0.100	0.244	0.058	0.039
D-7	0.351	0.250	0.096	0.246
D-6	0.350	0.353	0.077	0.277
G-2	0.098	0.502	0.062	0.019
H-1	0.200	0.499	0.104	0.096
D-11	0.350	0.499	0.171	0.177
*2D-12	0.350	0.500	0.289	0.050
I-1	0.464	0.501	0.148	0.315
D-5	0.351	0.635	0.178	0.157
D-3	0.351	0.758	0.205	0.129
H-2	0.198	0.981	0.123	0.060
I-2	0.470	1.013	0.276	0.176
D-2	0.350	1.505	0.199	0.136
D-1	0.350	2.006	0.209	0.116
		Annealed Low-Carbon Steel		
L-3	0.099	0.239	0.045	0.056
B-1	0.218	0.245	0.058	0.162
C-8	0.196	0.352	0.085	0.112
L-4	0.099	0.502	0.066	0.033
C-5	0.199	0.500	0.121	0.074
*2C-12	0.198	0.500	0.169	0.012
*2E-12	0.351	0.500	0.300	0.038
K-1	0.486	0.498	0.167	0.322
P-1	0.552	0.518	0.178	0.373
O-1	0.650	0.521	0.189	0.455
N-9	0.751	0.522	0.181	0.529
J-4	0.956	0.492	0.239	0.660
*Y-4	0.936	0.500	0.326	0.584
L-6	0.099	0.760	0.080	0.020
B-3	0.356	0.754	0.216	0.134
*K-14	0.450	0.747	0.404	0.047
P-8	0.552	0.770	0.287	0.249
O-12	0.648	0.772	0.206	0.437

TABLE 4 (Continued)

Plate Designation	Original Plate Thickness (inch)	C-3 Explosive Thickness (inches)	**Depth of Zone "A" (inch)	**Depth of Zone "B" (inch)
	Annealed Low-Carbon Steel (Continued)			
N-10	0.752	0.772	0.276	0.470
*J-17	0.956	0.747	0.594	0.312
K-9	0.486	0.852	0.281	0.190
*1C-12	0.198	1.026	0.179	0.013
B-5	0.356	0.991	0.268	0.083
*1E-12	0.351	1.026	0.308	0.014
*K-15	0.450	1.009	0.320	0.071
*K-7	0.486	1.016	0.320	0.146
P-2	0.552	1.010	0.304	0.225
*P-9	0.552	1.009	0.358	0.147
O-3	0.648	1.009	0.288	0.345
*O-2	0.650	1.005	0.554	0.064
R-3	0.851	1.019	0.420	0.439
*R-5	0.851	0.997	0.649	0.157
J-15	0.956	0.985	0.427	0.481
*X-4	0.936	1.026	0.687	0.135
*J-6	0.957	1.029	0.780	0.139
*J-9	0.956	1.016	0.730	0.158
B-2	0.198	1.497	0.134	0.063
B-6	0.356	1.504	0.225	0.102
*B-7	0.355	1.507	0.319	0.013
P-3	0.552	1.509	0.364	0.136
*P-10	0.552	1.515	0.494	0.039
O-4	0.648	1.522	0.359	0.242
N-3	0.749	1.502	0.422	0.298
*N-11	0.751	1.514	0.669	0.061
R-4	0.847	1.516	0.506	0.314
J-22	0.956	1.500	0.567	0.364
*J-10	0.956	1.516	0.814	0.062
C-6	0.199	2.008	0.140	0.046
E-3	0.351	2.011	0.212	0.105
P-4	0.552	2.016	0.295	0.190
O-7	0.650	2.008	0.343	0.241
N-7	0.752	2.006	0.482	0.217

*Plane-Wave Initiation.

**The depth of or thickness of both zones does not add to the original plate thickness due to residual compression of the specimens after explosive loading.

TABLE 5

SUMMARY OF TENSILE STRENGTH AND HARDNESS DATA

Plate Designation	Test Zone	Tensile Strength psi	% Elongation	% Reduction in Area	Average Hardness As Measured R_B(1)	Average Hardness As Measured DPH(2)	Approximate Hardness Associated with the Tensile Strength(3) R_B	Approximate Hardness Associated with the Tensile Strength(3) DPH
B-8(4)	B	86,200	11	57	91	188	88.6	182*
B-8	B	88,000	11	57	91	188	89.5	186*
U(5)	B	84,100	Broke outside the gauge mark		89	179	87.6	177*
U	B	84,100	15	64	89	179	87.6	177*
B-8	A	111,100	7	42	99	245	98.7	244
B-8	A	118,300	8	47	99	245	101.7*	260
U	A	117,200	8	42	99	236.5	101.4*	257.5
U	A	112,300	8	48	99	236.5	99.1	246.5
			Average Values					
B-8	B	87,100	11	57	91	188	89	184*
U	B	84,100	--	--	89	179	87.6	177*
B-8	A	114,700	7.5	44.5	99	245	99.7	250.5
U	A	114,750	8	45	99	236.5	99.7	250.5

(1) Rockwell Hardness Tester, B scale; 1/16 in. Ball penetrator - 100 kg load.

(2) Diamond Pyramid Hardness, 136° diamond indenter - 500 gram load.

(3) Values obtained from hardness conversion tables. Wilson Chart 5R issued by the Wilson Mechanical Instrument Division of the American Chain and Cable Company, Inc., was used to obtain the values of R_B and DPH not marked with an asterisk. Those values marked with an asterisk were obtained from Table 4 of ASTM Designation: E140-58. Because of the unusually wide range of hardnesses and the limits of tables available, some interconversion and extrapolation of hardness scales was necessary, hence the values given should not be considered exact. Conversion tables themselves are not exact.

(4) 1"0 annealed low-carbon steel, 1"5 C-3 oblique stress wave.

(5) 1"0 unannealed low-carbon steel, 1"0 C-3 oblique stress wave.

APPENDIX C

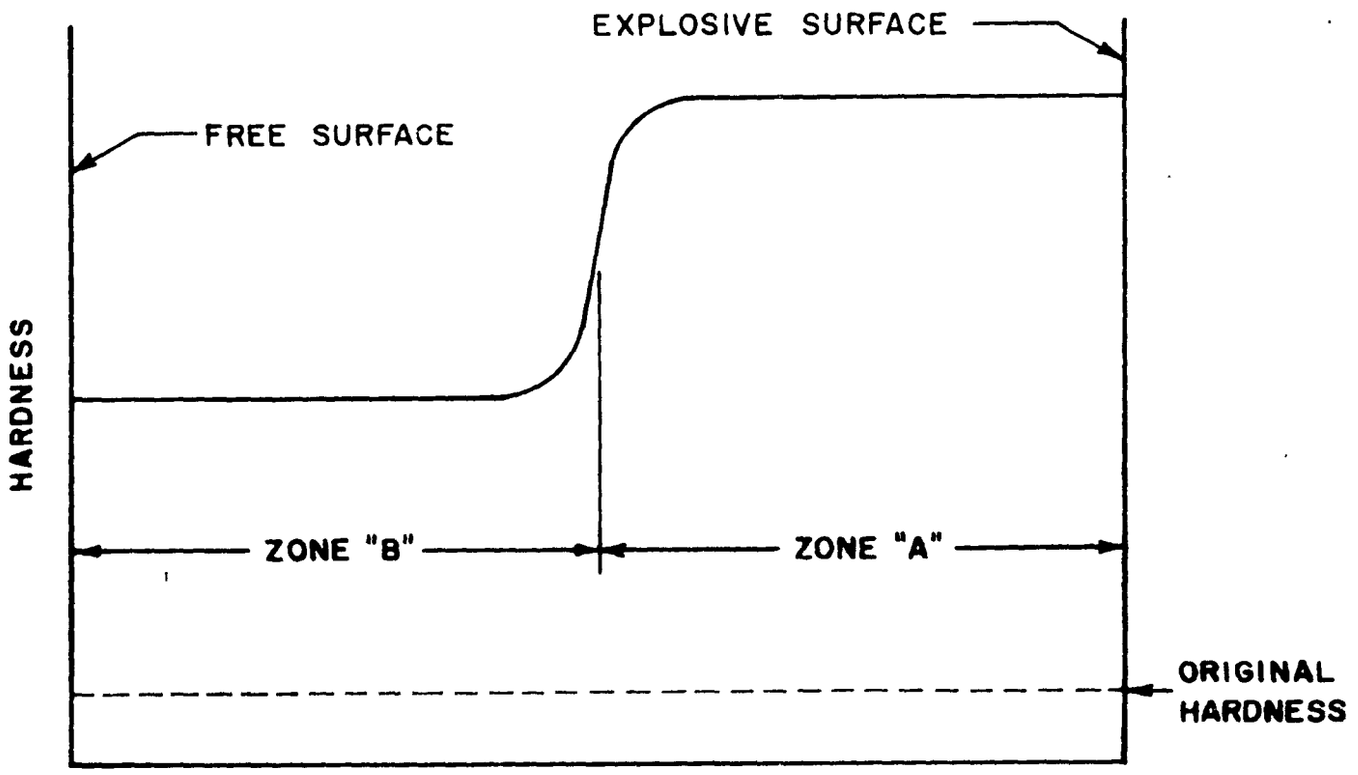

TYPICAL HARDNESS DISTRIBUTION THROUGH MILD STEEL PLATE AFTER EXPLOSIVE LOADING

FIGURE 1

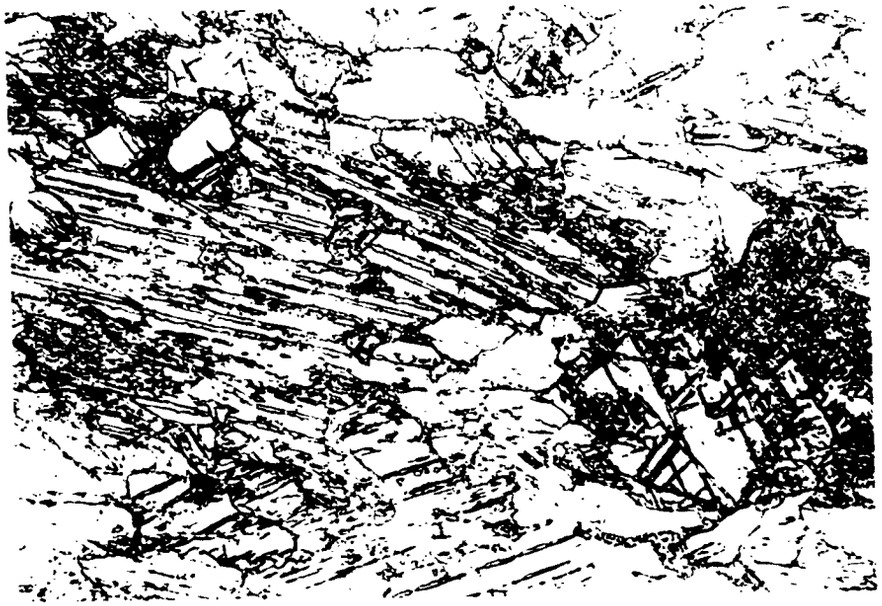

Typical microstructure of Zone A in steel (Etchant [illegible])

Typical microstructure of Zone [illegible] (Etchant [illegible])

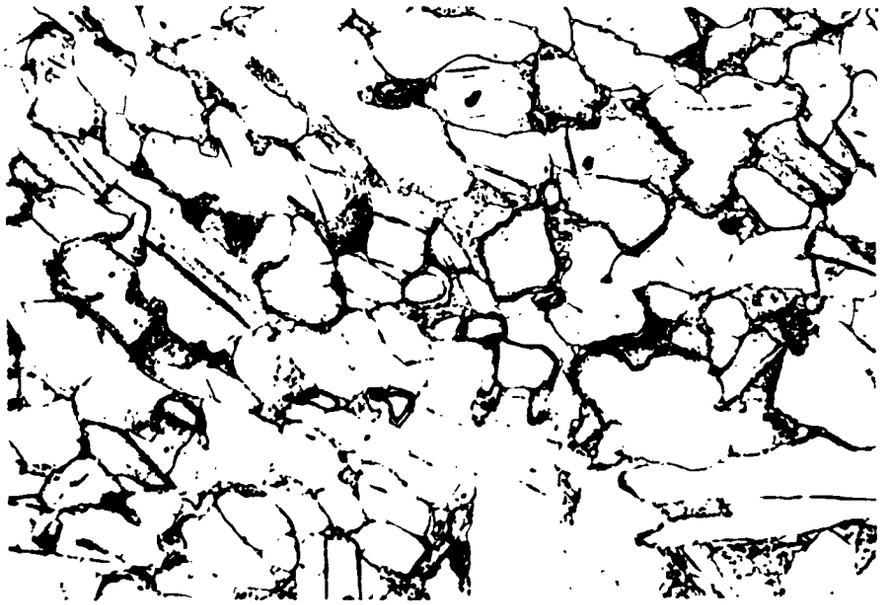

Typical Microstructure of Zone "B" in Steel (Plate K-6) 500X

Typical Weldor Structure of Zone "B" in Steel (Plate K-6) 500X

FIGURE 35

TYPICAL MICROSTRUCTURE OF ZONE "B"

ZONE "B"

ZONE "A"

Microstructure of Transition Region in Steel (Plate K-6) 500X

ZONE "B"

ZONE "A"

Microstructure of Transition Region in Steel (Plate K-6) 500X

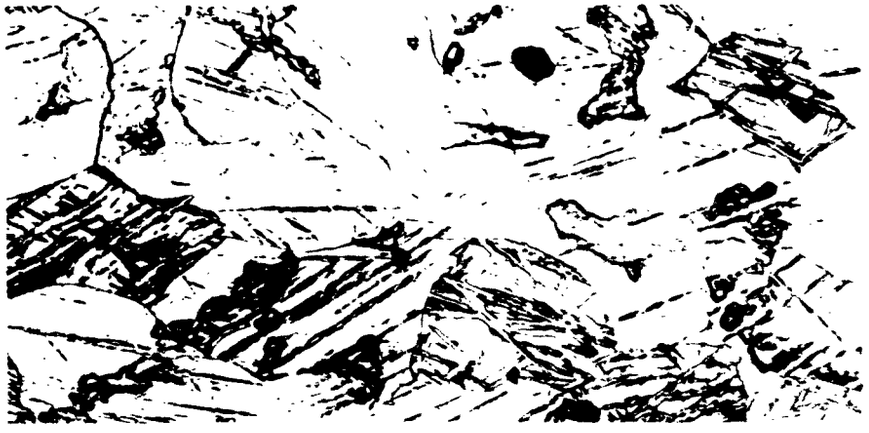

Microstructure of Transition Region in Steel (Plate K-6) 500X

HEDL-7771-11-84

FIGURE 3

TYPICAL MICROSTRUCTURE OF THE TRANSITION REGION

EXPLOSIVE CHARGE ASSEMBLIES

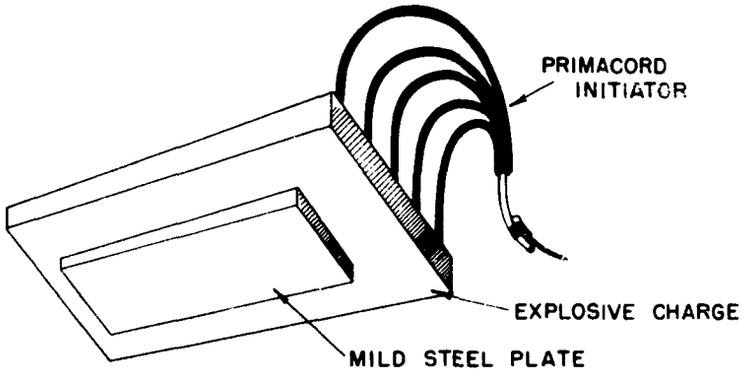

FIGURE 4a

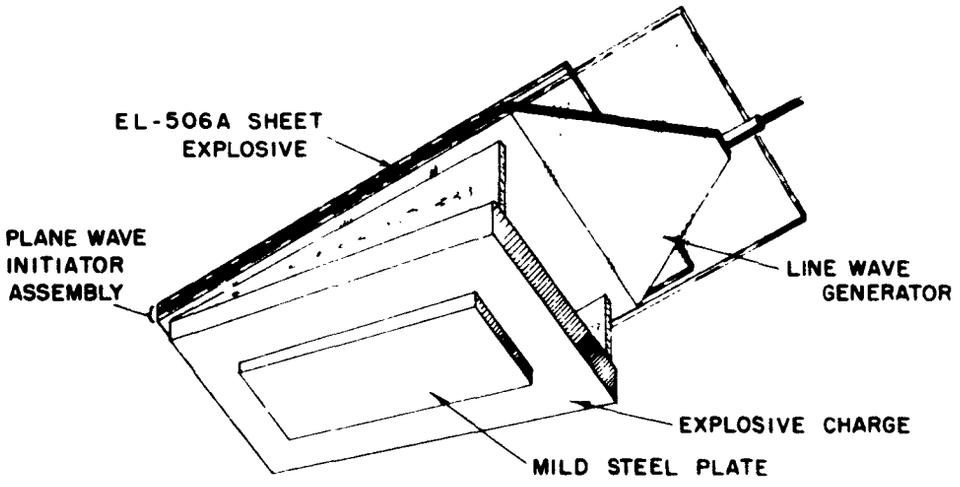

FIGURE 4b

PHD-55619

FIGURE 5

TYPICAL FIELD SET-UP OF A ROUND PRIOR TO FIRING

Free surface shown, left; explosive surface, right.

PHD-1772-11-64

FIGURE 6

TYPICAL PLATES AFTER LOADING

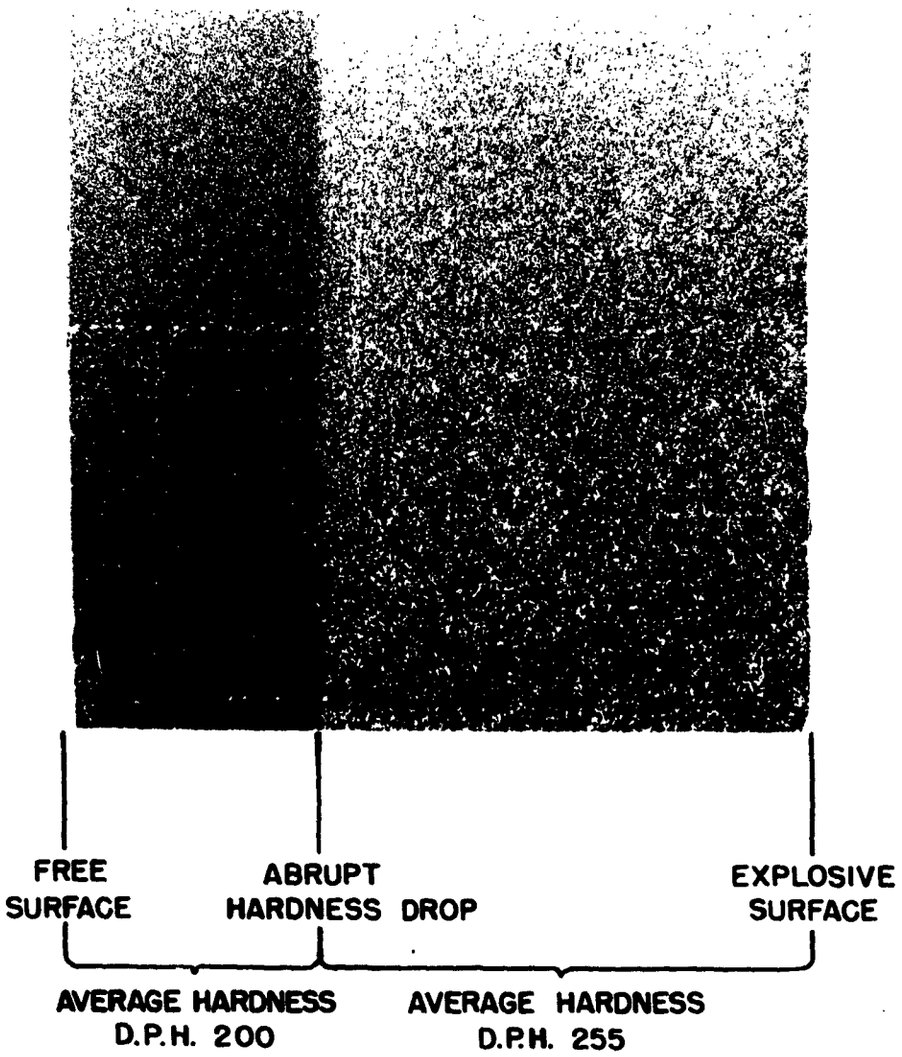

PHD-55482

FIGURE 7

ETCHED CROSS - SECTION OF SAMPLE PLATE

MAGNIFICATION: 10X

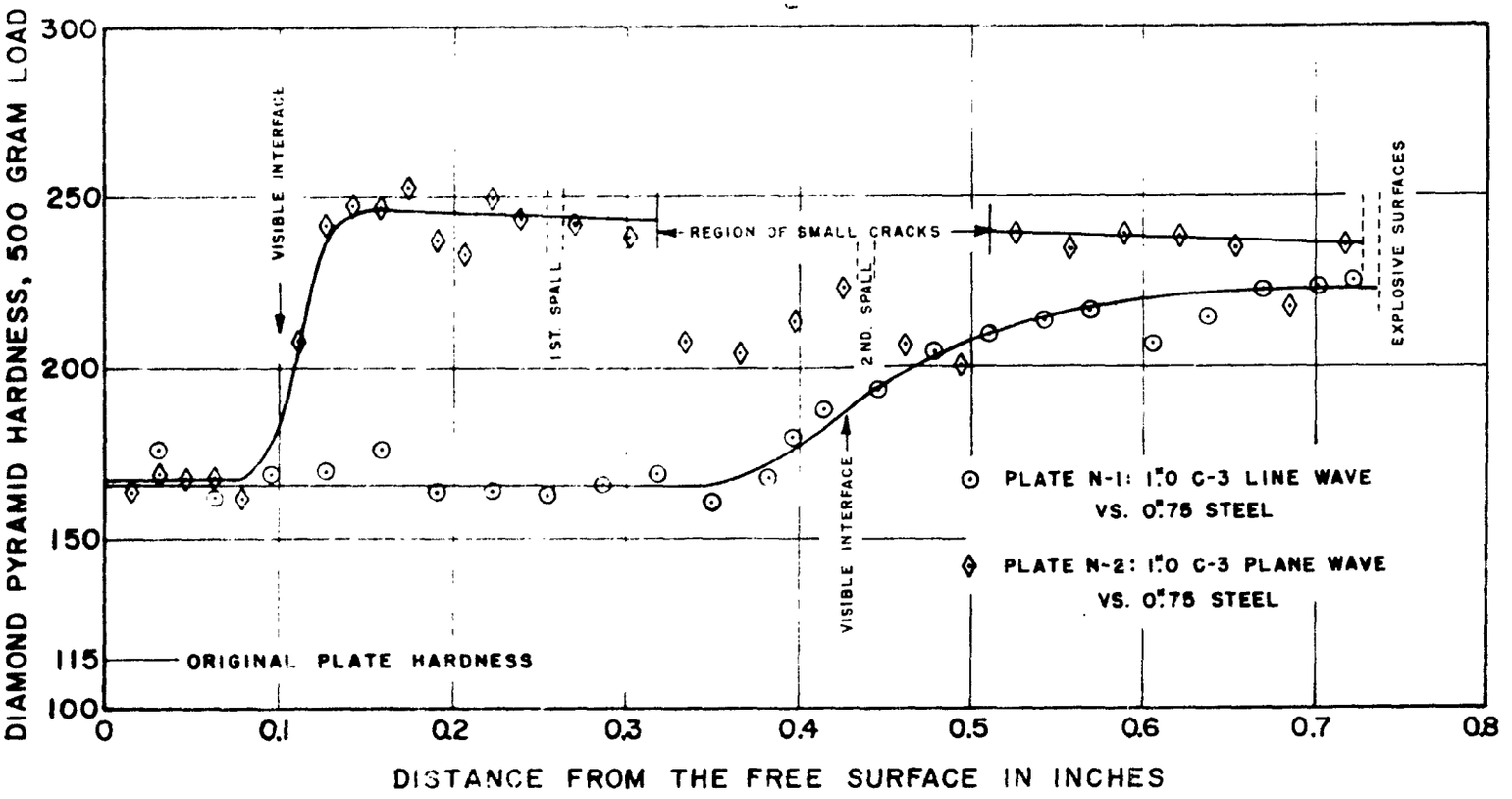

FIGURE 8: HARDNESS TRAVERSES THROUGH PLATES N-1 & N-2

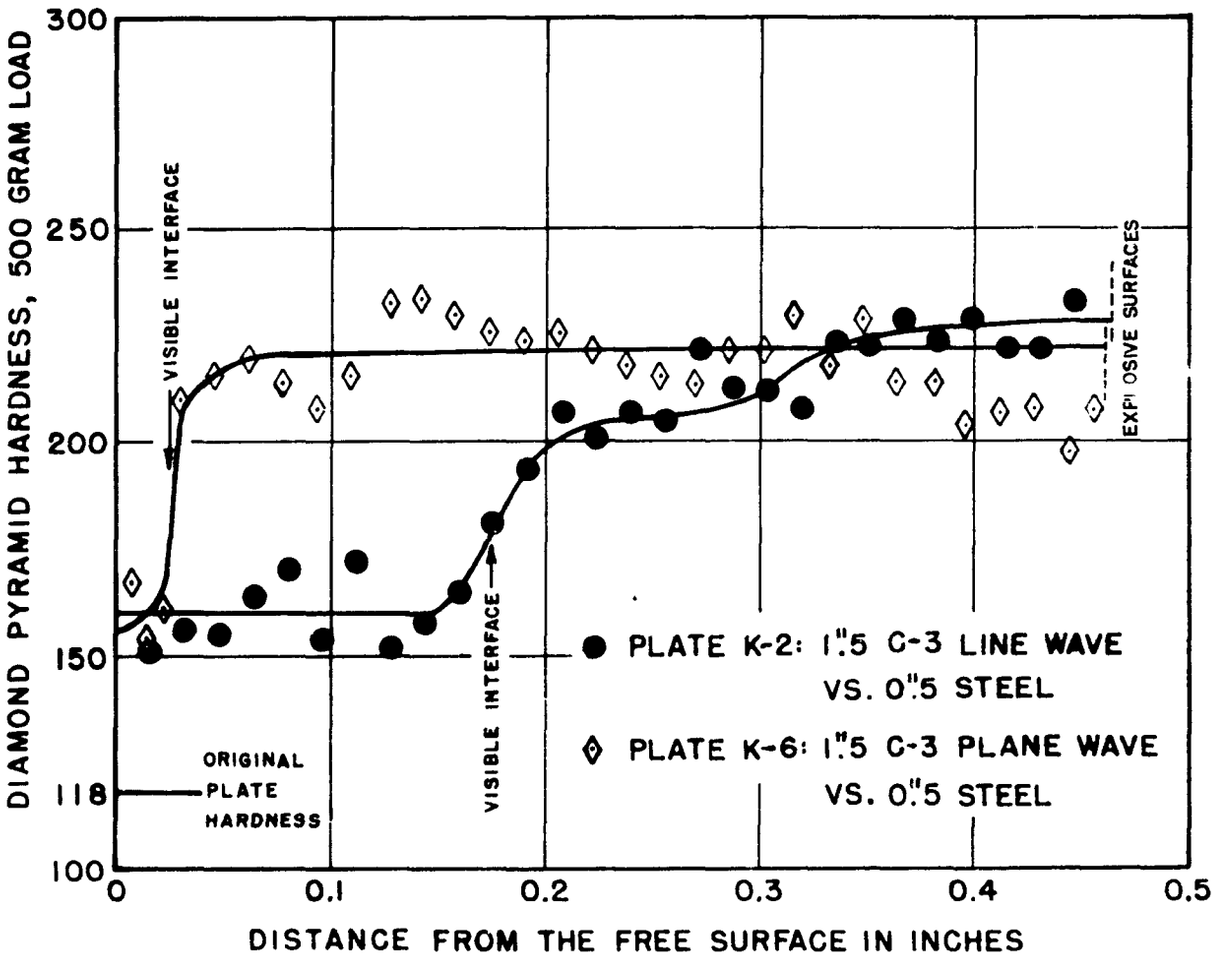

FIGURE 9: HARDNESS TRAVERSES THROUGH PLATES K-2 & K-6

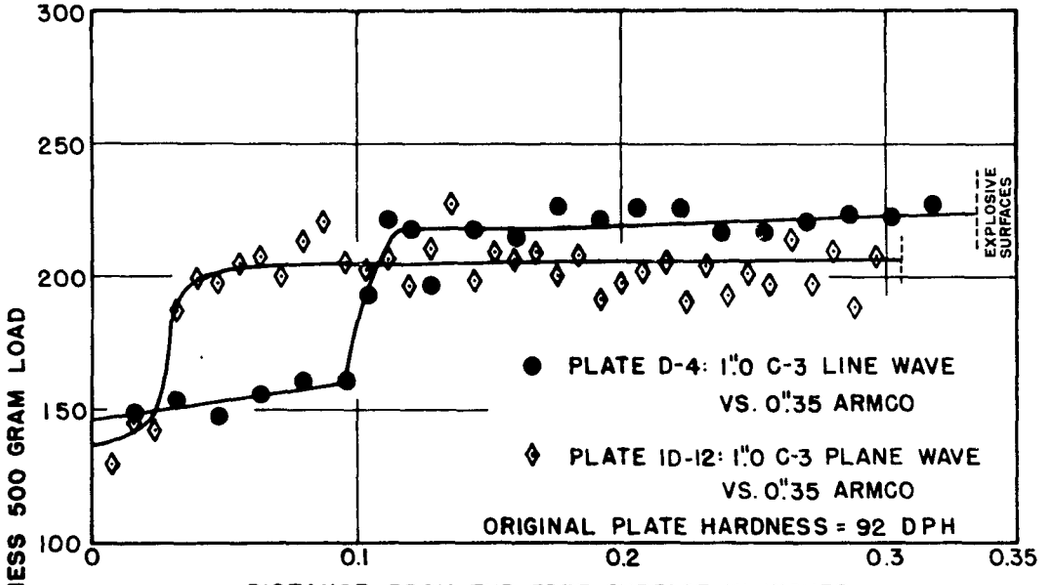

FIGURE 10A: HARDNESS TRAVERSES THROUGH PLATES D-4 & ID-12

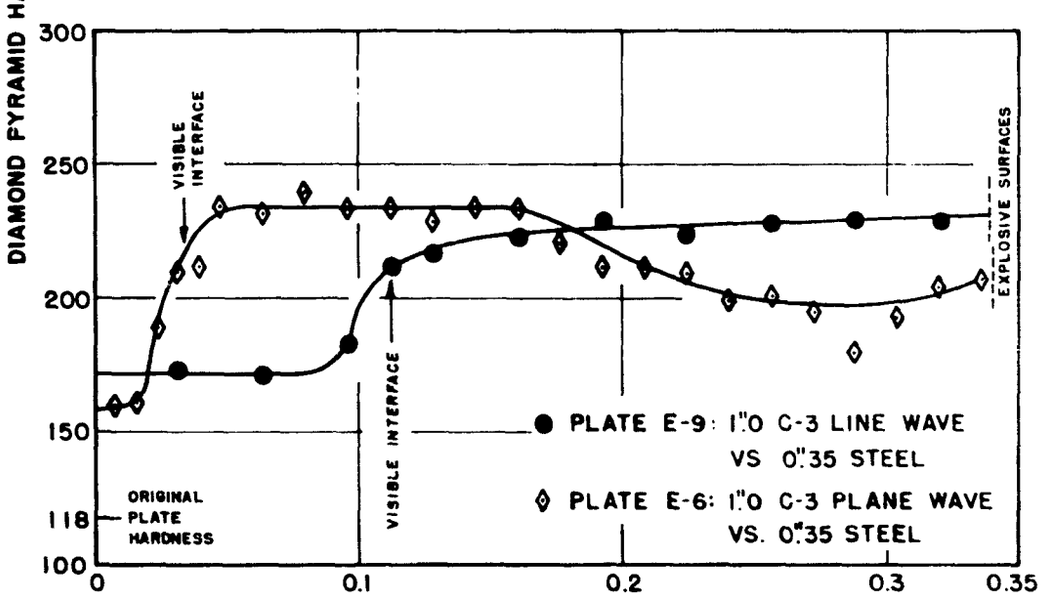

FIGURE 10B: HARDNESS TRAVERSES THROUGH PLATES E-6 & E-9

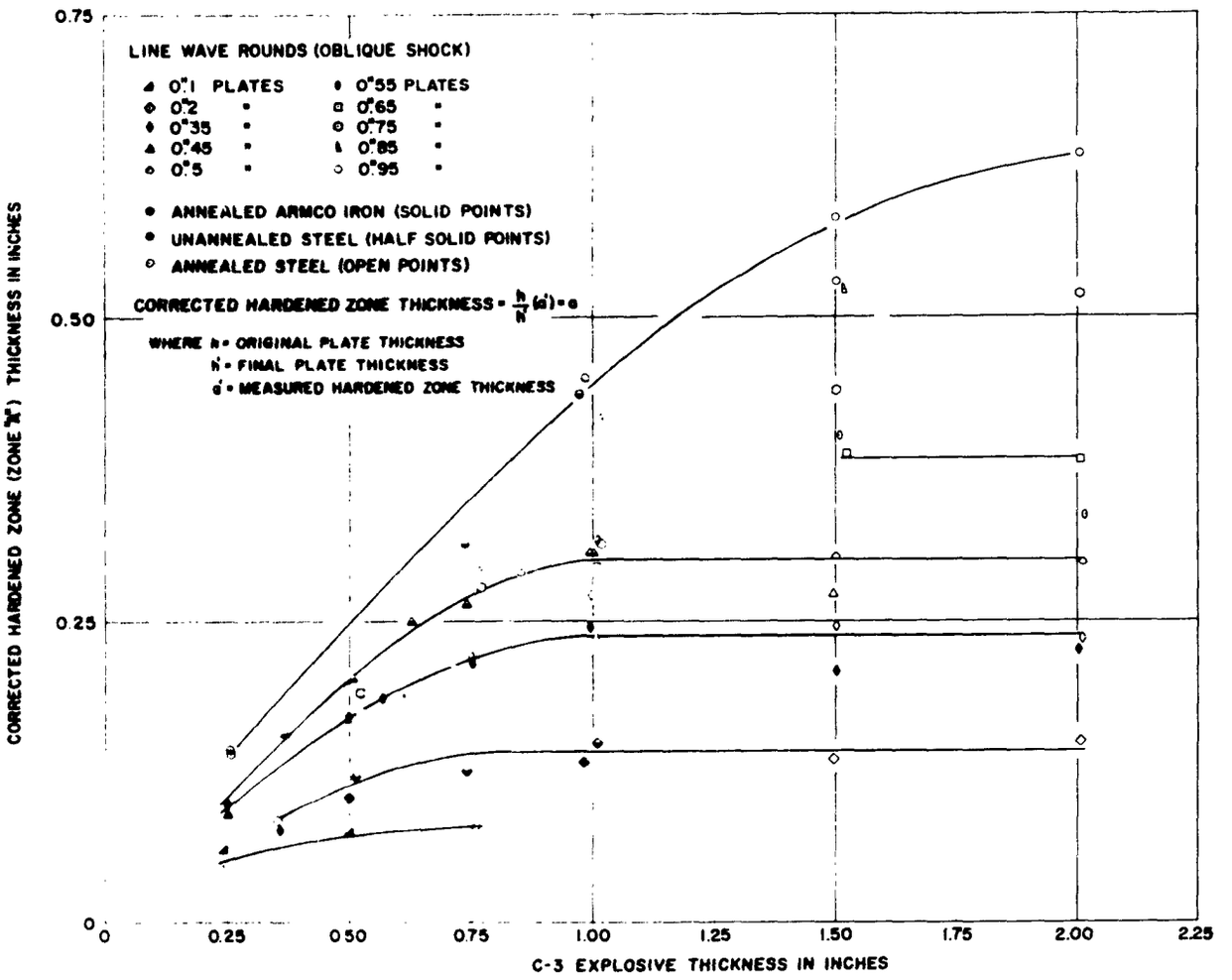

FIGURE 11. HARDENED ZONE THICKNESS VS. EXPLOSIVE THICKNESS

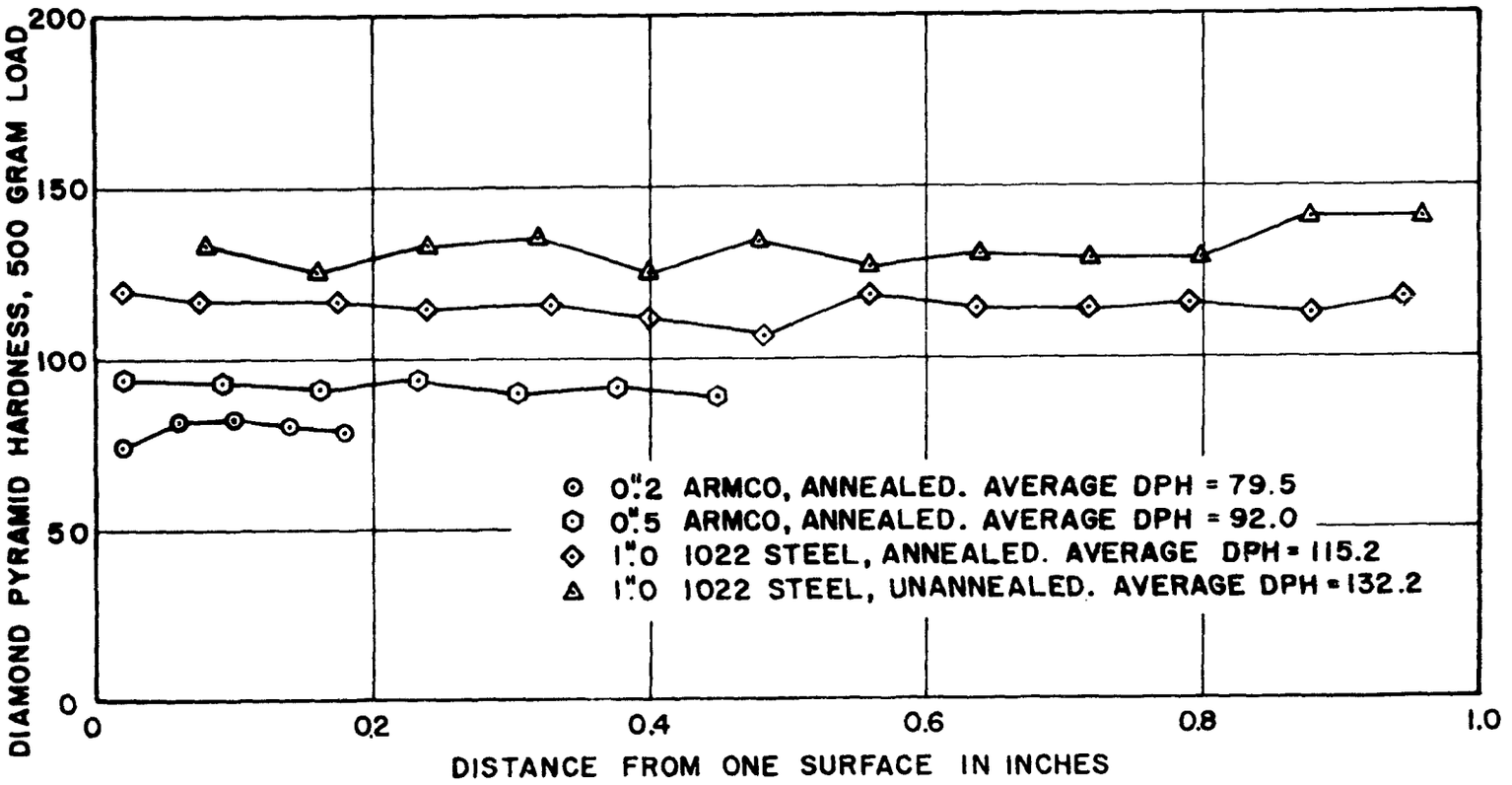

FIGURE 12: HARDNESS TRAVERSES OF UNLOADED STEEL AND ARMCO

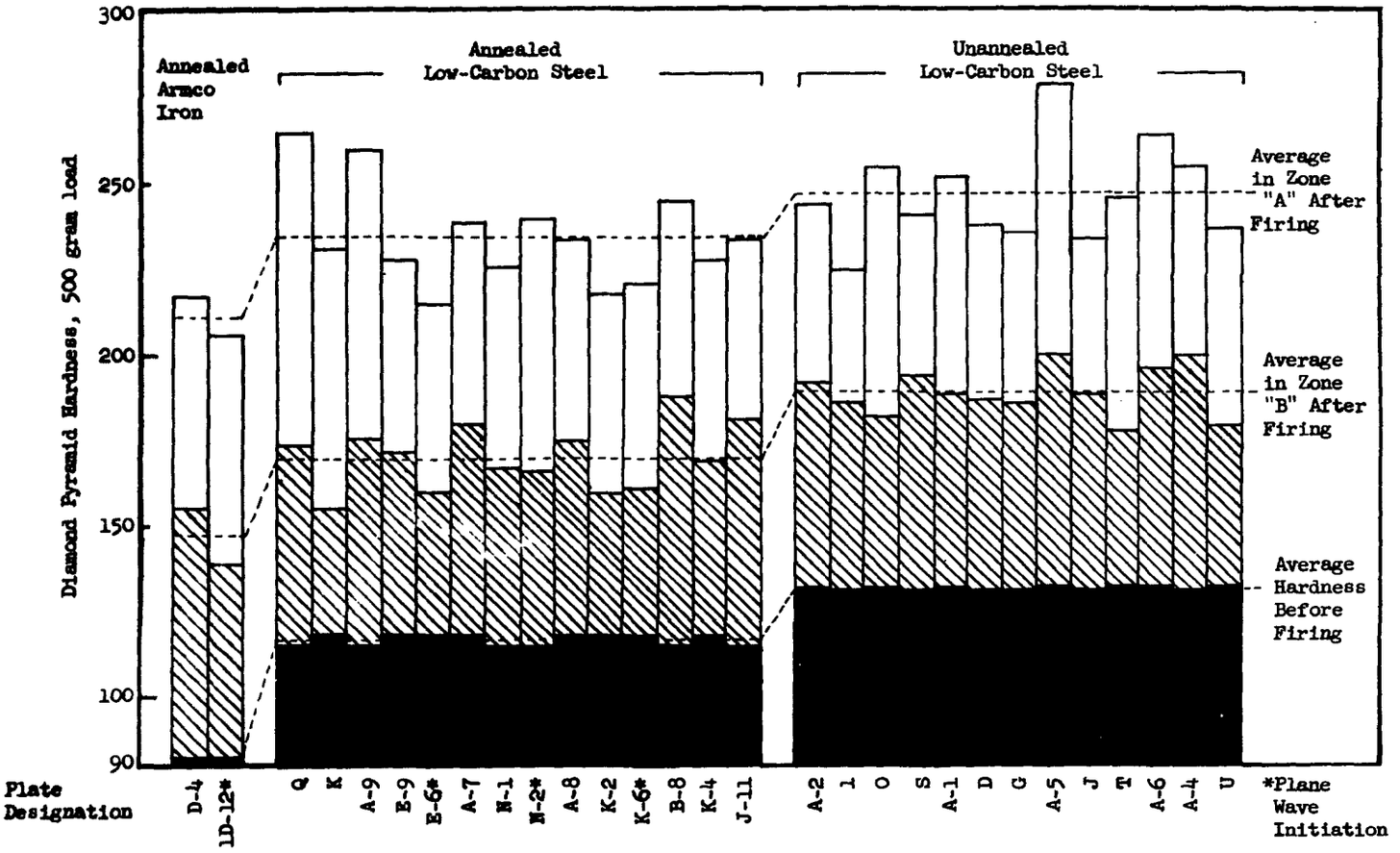

Figure 13. Effect of Original Hardness on Explosive Hardening

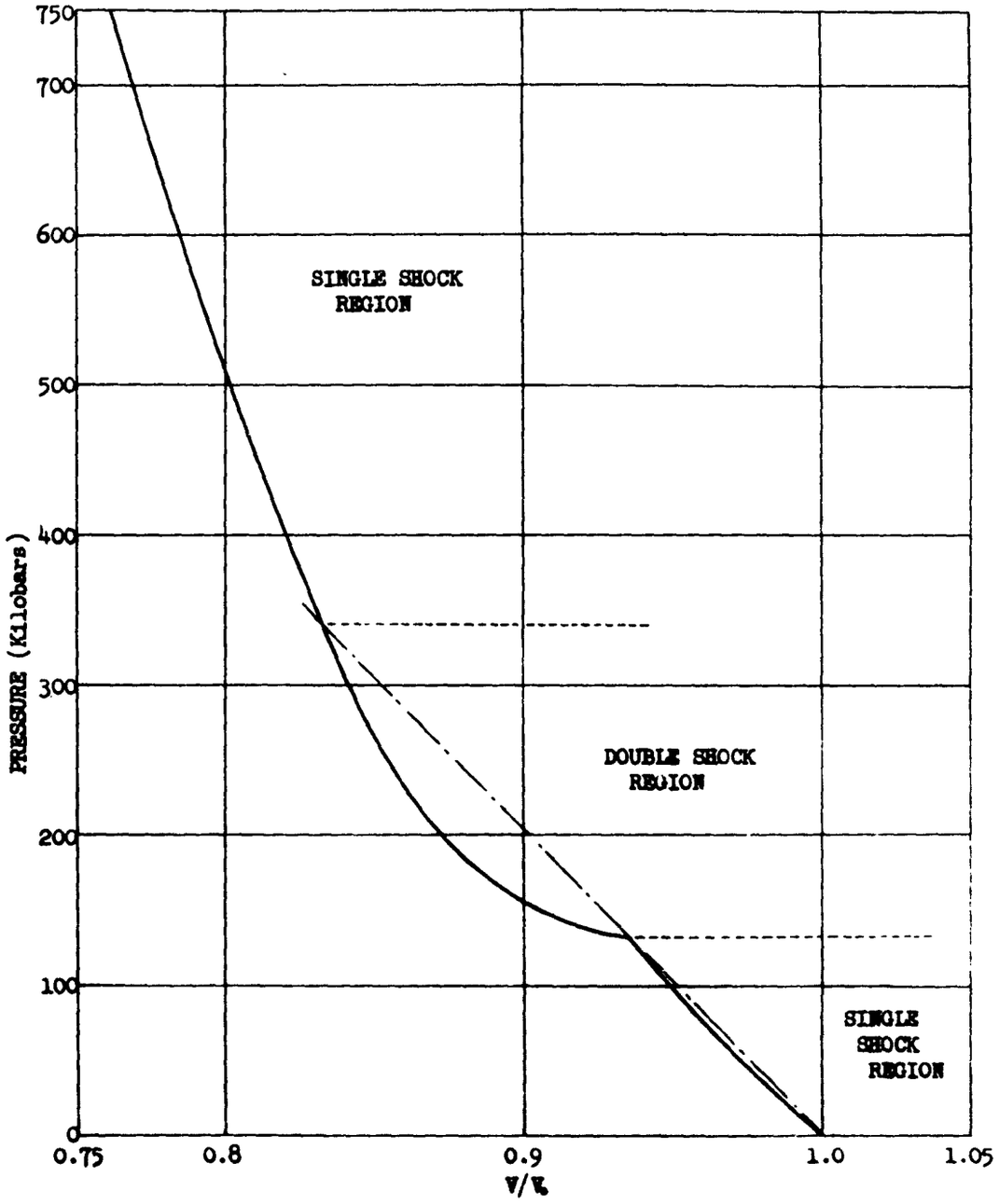

FIGURE 14: HUGONIOT CURVE FOR IRON.
(After Walsh et al., Ref. 14 and McQueen and Marsh, Ref. 15.)

APPENDIX D

DISTRIBUTION

Bureau of Naval Weapons:

DLI-31	2
RMMO-13	1
RMMO-422	1
RMMO-5	1
RRMA-2	1
RUME-11	1
RUME-4	1

Defense Documentation Center
Cameron Station
Alexandria, Virginia — 20

Commanding General
Aberdeen Proving Ground
Aberdeen, Maryland
Attn: Technical Information Section
Development and Proof Services — 2
Attn: Library — 1
Attn: BRL — 1

Commander, Operational Test and Evaluation Force
Norfolk 11, Virginia — 2

Commander
U. S. Naval Ordnance Laboratory
White Oak, Silver Spring, Maryland
Attn: Library — 1
Attn: ED Division — 1

Commander
U. S. Naval Ordnance Test Station
China Lake, California
Attn: Technical Library Branch — 1
Attn: Mr. John Pearson — 1

Commander
U. S. Naval Ordnance Test Station
Pasadena Annex
Pasadena, California
Attn: Library — 1

DISTRIBUTION (Continued)

Director
U. S. Naval Research Laboratory
Anacostia 20, D. C.
Attn: Library 1

Commanding Officer
Offite of Ordnance Research
Box CM, Duke Station
Durham, North Carolina 1

Commanding Officer
Picàtinny Arsenal
Dover, New Jersey
Attn: Library 2

Commanding General
Frankford Arsenal
Philadelphia 37, Pennsylvania
Attn: Technical Library 1

Commander
U. S. Naval Nuclear Ordnance Evaluation Unit
Kirtland Air Force Base
Albuquerque, New Mexico
Attn: Mr. E. B. Massengill 1

Commander
U. S. Air Force Special Weapons Center
Kirtland Air Force Base
Albuquerque, New Mexico
Attn: Library 1

Director, Applied Physics Laboratory
Johns Hopkins University
8621 Georgia Avenue
Silver Spring, Maryland
Attn: Library 2

Director
Los Alamos Scientific Laboratory
Los Alamos, New Mexico
Attn: Dr. C. M. Fowler 1
Attn: Library 1

DISTRIBUTION (Continued)

Battelle Memorial Institute
Defense Metals Information Center
Columbus 1, Ohio 2

The Institute for the Study of Rate Processes
University of Utah
Salt Lake City, Utah
Attn: Explosive Research Group 1

Stanford Research Institute
Poulter Laboratories
Menlo Park, California
Attn: Library 1

Director
Franklin Institute
20th Street and Benjamin Franklin Parkway
Philadelphia 3, Pennsylvania 1

Dr. G. E. Duvall
University of Washington
Seattle, Washington 1

The International Nickel Company, Incorporated
67 Wall Street
New York 5, New York
Attn: Mr. C. G. Bieber, Bayonne Research Laboratory 1
Attn: Dr. R. F. Decker, Bayonne Research Laboratory 1

New Mexico Institute of Mining and Technology
Socorro, New Mexico 1

Aerojet-General Corporation
Azusa, California 1

Institute for the Study of Metals
The University of Chicago
5640 Ellis Avenue
Chicago 37, Illinois
Attn: Dr. C. S. Smith 1

DISTRIBUTION (Continued)

British Joint Services Mission
The BNS/MOSS Scientific and Technical Information Section
P. O. Box 680, Benjamin Franklin Station
Washington, D. C.
Attn: Technical Information Center
Via: BUWEPS (DSC) 4

Defense Research Member
Canadian Joint Staff (W)
2450 Massachusetts Avenue, N. W.
Washington 8, D. C.
Attn: Dr. H. P. Tardiff, CARDE, Quebec (1)
Via: BUWEPS (DSC) 4

Sandia Corporation
Sandia Base
Albuquerque, New Mexico
Attn: Dr. F. W. Neilson 1

Sandia Corporation
Livermore, California
Attn: Technical Library 1

U. S. Department of Commerce
Coast and Geodetic Survey
Washington 25, D. C. 1

E. I. duPont de Nemours and Company, Incorporated
Wilmington, Delaware
Attn: Dr. G. E. Dieter 1

Local:

T	1
TD	1
TDMM-3	1
TDMM-4	1
TDP	1
TE	1
TE-2	1
TR	1
TRP	1
TRE-1	1
TRE-2	5
ACL	6
File	1

UNCLASSIFIED

Security Classification

DOCUMENT CONTROL DATA - R&D

(Security classification of title, body of abstract and indexing annotation must be entered when the overall report is classified)

1. ORIGINATING ACTIVITY *(Corporate author)* Naval Weapons Laboratory	2a. REPORT SECURITY CLASSIFICATION UNCLASSIFIED 2b. GROUP

3. REPORT TITLE

EXPLOSIVE HARDENING OF IRON AND LOW-CARBON STEEL.

4. DESCRIPTIVE NOTES *(Type of report and inclusive dates)*

5. AUTHOR(S) *(Last name, first name, initial)*

L. A. Potteiger

6. REPORT DATE	7a. TOTAL NO. OF PAGES	7b. NO. OF REFS
14 October 1964	13	

8a. CONTRACT OR GRANT NO.	9a. ORIGINATOR'S REPORT NUMBER(S)
b. PROJECT NO.	1950
c.	9b. OTHER REPORT NO(S) *(Any other numbers that may be assigned this report)*
d.	

10. AVAILABILITY/LIMITATION NOTICES

Qualified requesters may obtain copies of this report direct from DDC.

11. SUPPLEMENTARY NOTES	12. SPONSORING MILITARY ACTIVITY

13. ABSTRACT

The degree and depth of shock hardening in iron and low-carbon steel plates was experimentally determined by detonating C-3 explosive against the plates. Final hardness levels were strongly influenced by the magnitude of the pressure above the critical value of 130 kilobars or by explosive thickness or plate thickness, but were dependent upon the original hardness of the plate. The relative widths of the two hardness plateaus through the plate were found to depend upon explosive thickness, plate thickness, and applied pressure; a simple explanation for this dependence is presented in terms of the interaction of two shocks in the metal. The relationship of hardness and tensile strength was found to be about the same whether hardening was done explosively or by cold-working.

DD FORM 1 JAN 64 1473

UNCLASSIFIED

Security Classification